Curcumin Derivatives to Combat COVID-19:
A Computational Perspective

Dr. Adikay Sreedevi, M. Pharm, Ph.D

Professor
Institute of Pharmaceutical Technology
Sri Padmavati Mahila Visvavidyalayam, Tirupati, A.P, India

Dr.Kaveripakam Sai Sruthi, M. Pharm, Ph.D

Assistant professor (Contract)
Institute of Pharmaceutical Technology
Sri Padmavati Mahila Visvavidyalayam, Tirupati, A.P, India

Ms. Chintam Vasavi, B.Pharm
Ms. G.Sireesha, M.Pharm

Sri Padmavathi Mahila Visvavidyalayam,Tirupati, A.P, India

I   **Publisher**

Curcumin Derivatives to Combat COVID19: A Computational Perspective

Publication Year: November, 2023

MRP: INR 700

Contents

Chapter-I

Curcuminoids-Structures, Sources, Biological Activities and Curcumin Derivatives

Phytochemicals constitute naturally occurring chemical substances found in plants that are beneficial to human health and nutrition (Hasler & Blumberg, et al., 1999). The most prevalent and largest group of phytochemicals in the plant kingdom is referred to as phenolic phytochemicals. Flavonoids, phenolic acids, and polyphenols make up the three most significant dietary phenolic subgroups. Curcumin and polyphenolic chemicals are found in linear diaryl heptane molecules known as curcuminoids (Cao et al. 2014).

The perennial plant turmeric (*Curcuma longa*), a member of the Zingiberaceae family, contains phenolic substances called curcuminoids in the roots. The condiment made from this root is well-liked for its pleasing colour, which ranges from orange to yellow. The majority of this India-native plant is currently grown in Asia's warm, humid tropical regions like China and Indonesia. Turmeric is a spice and a yellow colour used in traditional cuisine (Meng et al., 2018).

DISCOVERY OF CURCUMIN

The rhizomes of *C. longa*, a member of the Zingiberaceae family of plants, are used to extract the active component of the culinary spice turmeric, curcumin. About 200 years ago, Vogel and Pelletier reported isolating a "yellow colouring matter" from the rhizomes of *Curcuma longa*, and they gave it the name curcumin.

SOURCES

Plants in the Curcuma genus, a member of the Zingiberaceae family, produce curcuminoids. The earth is home to more than a hundred different species of the Curcuma genus, including *Curcuma longa, Curcuma manga, Curcuma heyneana,* and *Curcuma zanthorrhiza,* all of which serve as sources of the curcuminoids.

STRUCTURES OF CURCUMINOIDS

The curcuminoids are composed of curcumin, a diferuloylmethane with the chemical formula $C_{21}H_{20}O_6$, as well as its two derivatives, demethoxy curcumin and bis-demethoxy curcumin, which have the chemical formulas $C_{20}H_{18}O_5$ and $C_{19}H_{16}O_4$, respectively. They are structurally similar, consisting of two benzene methoxy rings connected by an unsaturated chain. The aromatic methoxy phenolic group, the,-unsaturated -diketo linker, and the keto-enol tautomerism are its three key roles. Both the R1 and R2 substituents on the curcumin are methoxy groups. Hydrogen and methoxy groups are the only substituents in the bisdemethoxycurcumin, but both are present in demethoxycurcumin. These substances are all available as trans-trans keto-enols. Hydrophobicity is provided by the aromatic groups, and flexibility is provided by the linker. The hydrophobicity and polarity are also influenced by the tautomeric structures. Curcuminoids are hydrophobic, which renders them little soluble in water
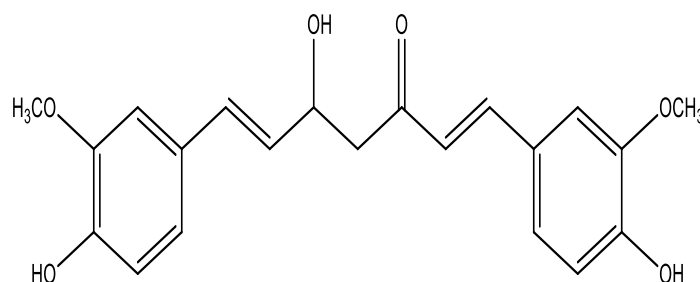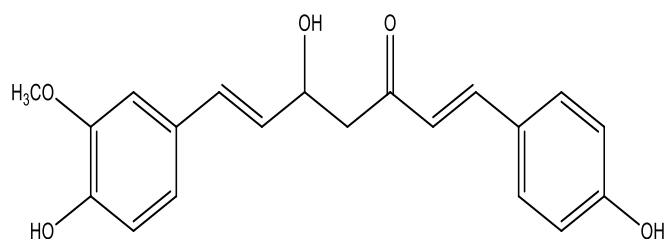

Figure A: Curcumin

Figure B: Dimethoxy Curcumin
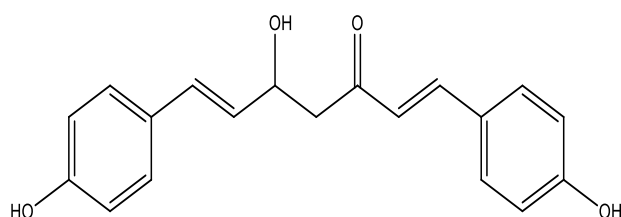
Figure C: Bisdemethoxy Curcumin

BIOLOGICAL ACTIVITIES (*Ferreira et al., 2022*) **:**
- Anti-Tumor
- Anti-inflammatory
- Anti-bacterial
- Anti-fungal
- Anti-viral
- Anti-protozoal
- Anti-diabetic
- Anti-oxidant

Pharmacokinetics properties of Curcumin
Studies on the pharmacokinetics as well as bioavailability of curcumin have revealed limited intestinal absorption. 400 mg of curcumin taken orally has an absorption rate of 60–66% and is quickly eliminated from the body. Due in significant part to its low solubility and quick metabolism, which results in low bioavailability, curcumin's clinical usage is restricted. It can pass across the blood-brain barrier.

Chapter-II

Review of literature

Curcumin is more accessible for research and drug development compared to other naturally sourced bioactive compounds that are present in low concentrations in the source plants. Curcumin possesses a wide range of biological effects and such versatility makes curcumin a promising lead compound for the development of new derivatives that may have a role in the management of numerous illnesses

Curcumin derivatives

The following are some of the evidences for the pharmacological activities of curcumin derivatives:

Dnyaneshwar et al., (2020) synthesized Amide-Linked Monocarbonyl Curcumin Analogues by Clasien-Schmidt reaction .They evaluated the synthesized derivatives for their *in vitro* antitubercular activity against *M. tuberculosis* by established XTT Reduction Menadione assay (XRMA) method and their results illustrated that these derivatives possess potent anti tubercular activity.
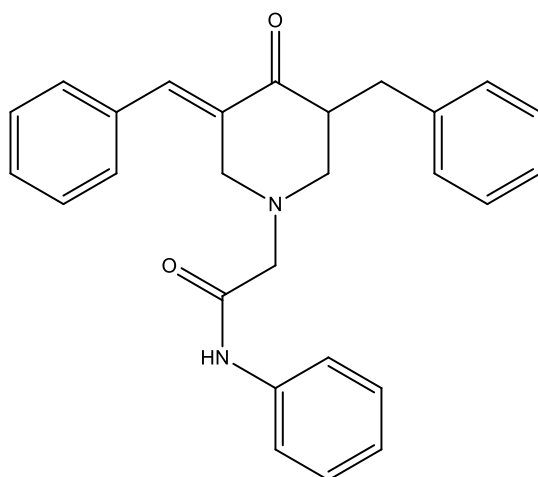
(*E*)-2-(3-benzyl-5-benzylidene-4-oxopiperidin-1-yl)-*N*-phenylacetamide

Singh et al.,(2019) synthesized triazole-tethered monocarbonyl curcumin− coumarin and curcumin−isatin molecular hybrids by eliminating its sensitive β-diketone moiety (responsible for its pharmacokinetic limitations) via several modifications in its parent structure to elevate its stability as well as bioavailability .Their results showed that these derivatives exhibit prominent antibacterial activity.
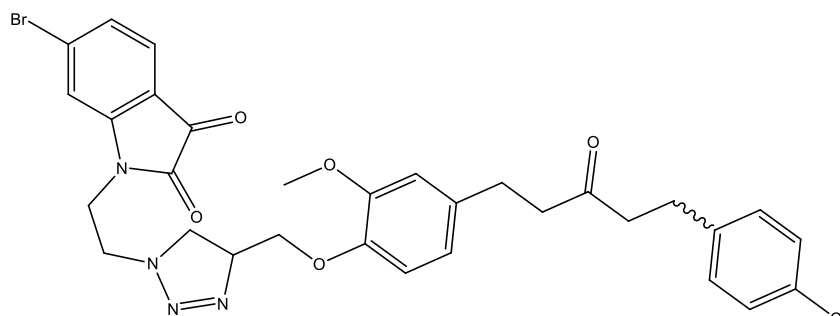
6-bromo-1-(2-(4-((4-(5-(4-chlorophenyl)-3-oxopentyl)-2-methoxyphenoxy)methyl)-4,5-dihydro-1*H*-1,2,3-triazol-1-yl)ethyl)indoline-2,3-dione

Kim et al.,(2018) synthesised novel curcumin compounds containing isoferuloyl and catechol moieties using acetylacetone with equivalent of corresponding aldehydes by Pabon's method. These compounds were evaluated for inhibitory effects on *S. pneumoniae* Nan A using a fluorescence (FL)-based assay. Their findings revealed that inhibitory effect on bacterial salidase increased with the greater substitution of hydroxyl groups in the phenyl rings.
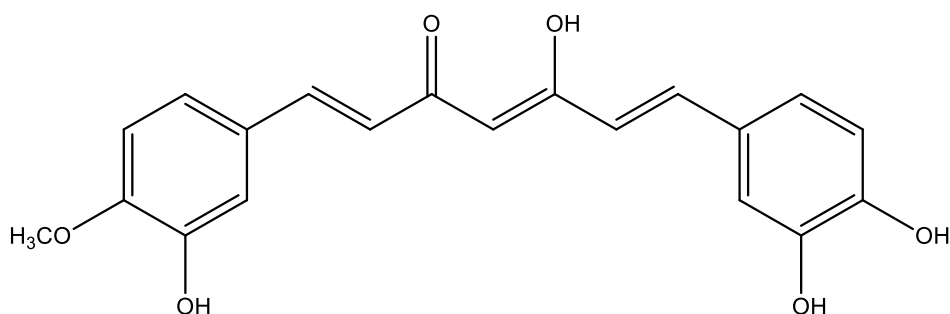
(1*E*,4*Z*,6*E*)-7-(3,4-dihydroxyphenyl)-5-hydroxy-1-(3-hydroxy-4-
methoxyphenyl)hepta-1,4,6-trien-3-one

Emam et al.,(2017) synthesized novel curcumin arylhydrazones analogues by Diazocoupling reaction of curcumin with different diazonium salts of *p*-toluidine, 2-aminopyridine, and 4-aminoantipyrine in pyridine . The compounds were tested for antioxidant activity using a 2,2-diphenyl-1-picrylhydrazyl (DPPH) assay and proved to have good antioxidant potential.
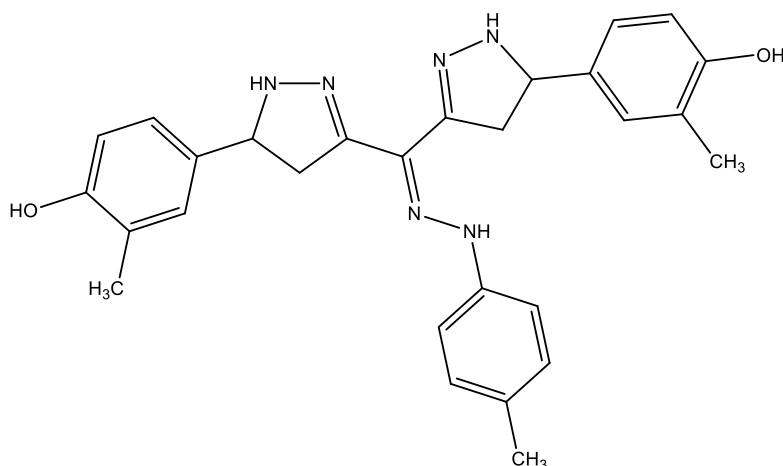
4,4'-(3,3'-((2-(*p*-tolyl)hydrazono)methylene)bis(4,5-dihydro-1*H*-pyrazole-5,3-diyl))bis(2-methylphenol)

Jaggi and his coworkers (2016) synthesized Curcumin 3,4-dihydropyrimidinones/thiones/imines using one-pot cyclocondensation of curcumin with substituted aromatic aldehydes and urea. These compounds were studied and found to possess anti- inflammatory activity and antioxidant activity.
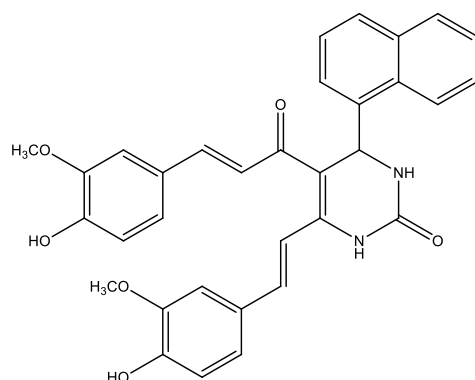
5-((*E*)-3-(4-hydroxy-3-methoxyphenyl)acryloyl)-6-((*E*)-4-hydroxy-3-methoxystyryl)-4-(naphthalen-1-yl)-3,4-dihydropyrimidin-2(1*H*)-one

Puneeth et al.,(2015) synthesized a series of curcumin pyrazole derivatives by base catalyzed cyclization of different phenyl hydrazines with curcumin in the existence of ethanol under reflux condition. Both electrons withdrawing and electron donating substituent's on phenyl hydrazines smoothly underwent cyclization with curcumin to generate pyrazole derivative. These compounds were evaluated for antioxidant activity and tested for free radicals scavenging activity in different *in-vitro* models.
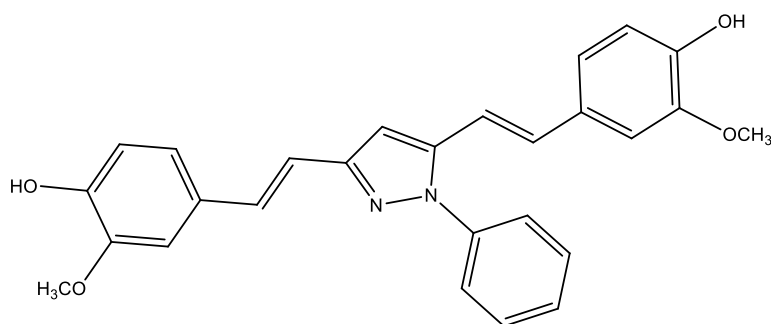

4,4'-((1*E*,1'*E*)-(1-phenyl-1*H*-pyrazole-3,5-diyl)bis(ethene-2,1-diyl))bis(2-methoxyphenol)

Yuan et al.,(2014) synthesized a series of mono-carbonyl analogues of curcumin by deleting the reactive beta-diketone moiety, which is responsible for the pharmacokinetic limitation of curcumin. These compounds were synthesized by coupling the appropriate aromatic aldehyde with cyclohexanone, cyclopentanone, acetone or piperidone in an alkaline medium. These analogues were evaluated for their antidiabetic activity by 11b-HSD2 assay in rat and found to possess prominent antidiabetic effect.
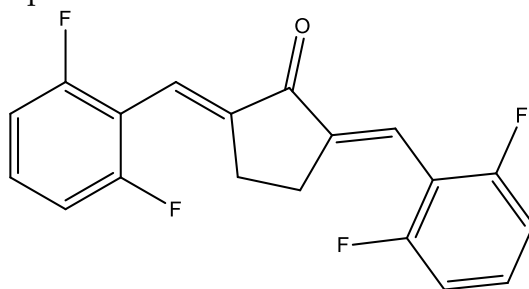
(2*E*,5*E*)-2,5-bis(2,6-difluorobenzylidene)cyclopentanone

7

Bingmi et al.,(2013) synthesized novel curcumin analogues with α,β-unsaturated ketone moiety and/or α,β-saturated ketone structure from curcumin via alkylation at the central carbon and the phenolic hydroxy groups, and hydrogenation of α,β-unsaturated ketone moiety. The antiproliferative activity of these curcumin analogues were evaluated and reported.
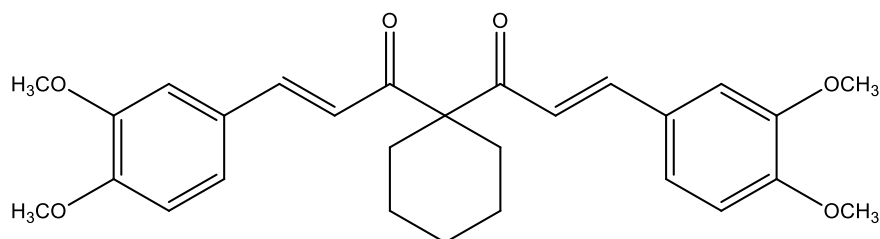
(2*E*,2'*E*)-1,1'-(cyclohexane-1,1-diyl)bis(3-(3,4-dimethoxyphenyl)prop-2-en-1-one)

Khan et al.,(2012) synthesized heterocyclic aromatic curcuminoids involving a reaction between the appropriate aldehyde and acetylacetone–boric anhydride complex. In these novel curcuminoid derivatives the researchers replaced the bis-methoxy-phenyl group of curcumin with bis-dimethoxy butenolidyl- (ascorbate), bis-naphthyl, and bis-furanyl derivatives, Further they studied and reported that these derivatives exhibited Anti-inflammatory activity using the standard carrageenan induced paw oedema assay.
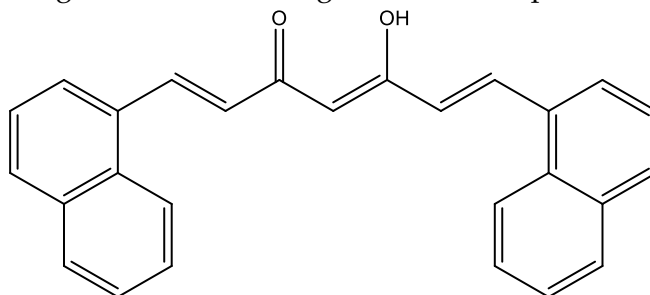
(1*E*,4*Z*,6*E*)-5-hydroxy-1,7-di(naphthalen-1-yl)hepta-1,4,6-trien-3-one

Shang-Ying et al., (2011) synthesized and reported the antioxidant activity of novel curcumin analogues by aldol condensation in which an N-methylpiperazine was introduced on the two aromatic ends .
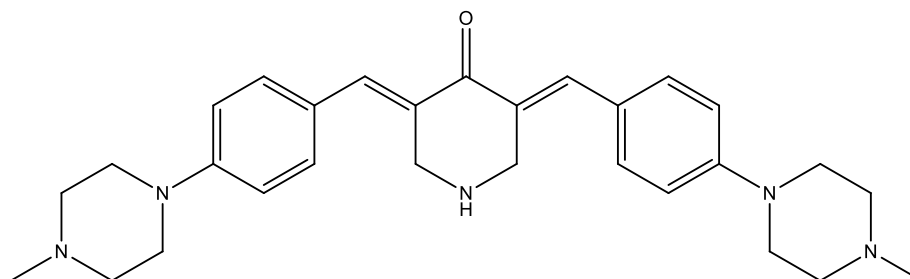
(3*E*,5*E*)-3,5-bis(4-(4-methylpiperazin-1-yl)benzylidene)piperidin-4-one

Ramendra et al.,(2010) synthesized curcumin biconjugate analogues using dicyclohexylcarbodiimide (DCC) coupling procedure in the presence of DMAP in anhydrous dichloromethane (DCM). These compounds were evaluated and reported for

their cytotoxicity and antiviral activity against a variety of DNA and RNA viruses using different cell cultures.

((1*E*,6*E*)-3,5-dioxohepta-1,6-diene-1,7-diyl)bis(2-methoxy-4,1-phenylene) dinonanoate
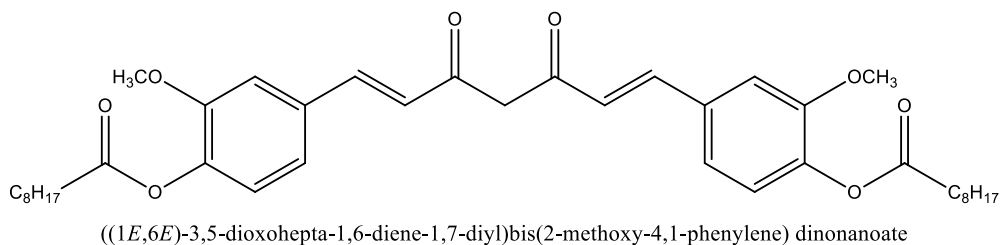
The literature mentioned above makes it abundantly clear that curcumin and its derivatives have a wide spectrum of biological functions. Additionally, it has been found that these compounds have strong antibacterial, antioxidant, anticancer, and antidiabetic properties.

Chapter-III

Virus, Types, SARs CoV-2, Epidemiology, Diagnosis and Treatment of COVID-19

VIRUS

The virus is a simple biosystem that exhibits certain characteristics of living systems, including having a genome and the capacity to adapt to changing environmental conditions. They differ from other microorganisms because to their minimal organisation, distinctive form of replication, and obligate parasitism. They are unable to capture and share free energy, are not actively functioning outside of their host cell, and can only exist as parasites. (Yolles et al. 2000).

TYPES OF VIRUSES

Viruses appear in a wide variety of sizes and shapes, but they are all formed of the same two basic parts: a core of genetic information, either DNA or RNA, that is encased in a capsid, a protective protein coating. Four shapes are available for a single virion:

1.Helical Viruses:

They have a slinky-shaped capsid that twists around and encloses its genetic material.

Examples: Rabies Virus, Ebola Virus

2.Polyhedral Viruses:

They are composed of genetic material surrounded by a many-sided capsid, usually with 20 triangular faces.

Example: Adeno virus

3.Spherical Viruses:

These viruses are essentially a helical virus enclosed in a membrane known as an envelope, which is spiked with sugary proteins that assist in sticking to and entering host cells.

Examples: Polio Virus, Herpesvirus, Corona Virus.

4.Complex Viruses:

These viruses resemble a lunar lander, and composed of a Polyhedral head and a helical body that attach to a cell membrane so that it can transfer its genetic material.
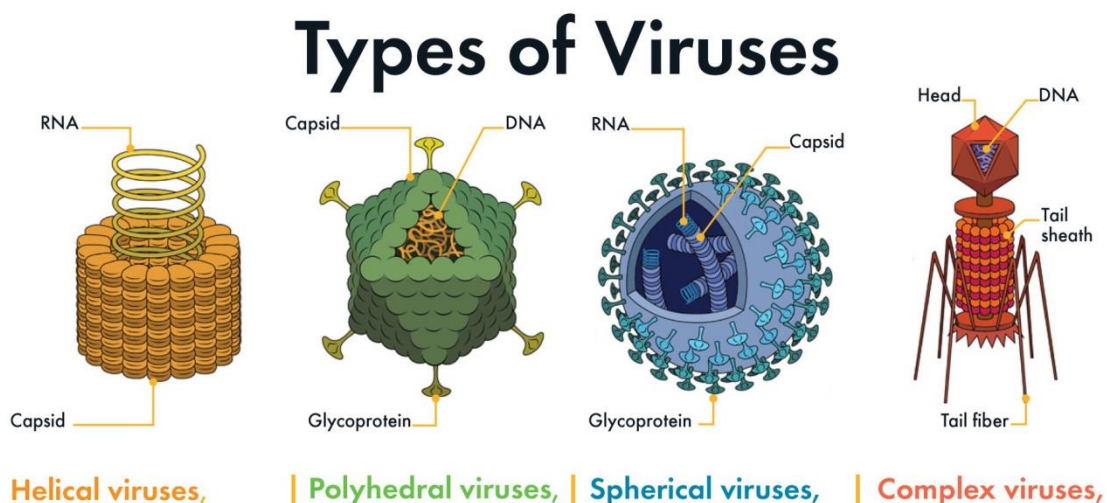
Examples: Pox Virus, Gemini Virus.

Figure 1: Different types of viruses (Harvard.edu)

VIRAL DISEASES

Viruses are extremely tiny infectious organisms. Any disease or condition brought on by a virus is referred to as a viral disease. Viral infections happen when a virus enters the body and invades the inside of the body's cells in order to proliferate. Viral diseases are

contagious. The virus multiplies and spreads to other cells if the body's immune system is unable to kill it, repeating the process and causing a widespread infection. Viral infections and viral illnesses can be caused by a range of different virus types. More than 200 distinct viruses have been found to mostly cause respiratory illnesses.

RESPIRATORY VIRUSES

Respiratory viruses are those that predominantly affect the respiratory tract. Due to their widespread frequency, significant morbidity and death, fast spread in communities, and mode of transmission (often by aerosol, direct contact, or by fomites), respiratory virus infections pose a serious threat to public health. 200 respiratory viruses affect people, with the majority belonging to the *Orthomyxo viridae, Paramyxo viridae, Picorna viridae, Corona viridae, Adeno viridae,* and *Herpes viridae* families.

Types of respiratory viruses:

Different types of respiratory viruses and their involvement in respiratory tract diseases are mentioned in Table 1.

Table 1: Involvement of different respiratory viruses in respiratory tract diseases

Virus	Common cold	Flu/flulike illness	Otitis media	Bronchiolitis	Pneumonia
Influenza	++++	++++	-	+	++++
Parainfluenza	+++	+	-	++++	++++
HRSV	+++	+	-	++++	++++
Adenovirus	+++	++	-	-	++++
Rhinovirus	++++	+	+	-	-
Coronavirus	++	+	+	-	+

+to++++ minimal or major importance, -no or negligible importance (clinical virology manaual´3rdedition, 2000)

SARS CoV-2:(SEVERE ACUTE RESPIRATORY SYNDROME CORONA VIRUS 2)

Severe Acute Respiratory Syndrome Coronavirus 2 (SARS-CoV-2) is a newest coronavirus that is responsible for Coronavirus Disease 2019 (COVID-2019). The SAR-CoV-2 virus belongs to the widely distributed sarbecovirus, ortho corona virinae subfamily and is an enveloped, non-segmented, positive sense RNA virus. Compared to other RNA viruses, CoVs have bigger genomes (27–32 kb), which are single-stranded positive-sense RNA (+ss RNA). The genome of the recently sequenced SARS-CoV-2 is around 29.9 kb in size. SARS-CoV-2 is composed of sixteen non-structural proteins (nsp1–16) in addition to the four primary structural proteins spike (S) glycoprotein, small envelope (E) glycoprotein, membrane (M) glycoprotein, and nucleocapsid (N). Nsp1 mediates RNA replication and processing. Nsp2 modifies the host cell's survival signalling system. The translated protein is thought to be separated by Nsp3. Nsp4 alters ER membranes and has transmembrane domain 2 (TM2). Nsp5 takes part in the replication-related polyprotein process. A presumed transmembrane domain is Nsp6. The interaction between nsp12 and template-primer RNA was greatly enhanced by the presence of nsp7 and nsp8. As a ssRNA-binding protein, Nsp9 serves a purpose. Nsp10 is essential for viral mRNA cap methylation. The RNA dependent RNA polymerase (RdRp), an essential component of coronavirus replication and transcription, is found in Nsp12. Nsp13 interacts with ATP, and its zinc-binding domain is

involved in transcription and replication. A proofreading exoribonuclease domain is Nsp14. Nsp15 has endoribonuclease activity that is Mn (2+) dependent. A 2'-Oribose methyltransferase is Nsp16. According to one study, NSP-mediated effects on protein trafficking, translation, and splicing can suppress host defences. NSP16 interacts to the U1 and U2 snRNAs' mRNA recognition domains after SARS CoV-2 infection to prevent mRNA splicing. In order to prevent mRNA from being translated, NSP1 binds to 18S ribosomal RNA in the mRNA entrance channel of the ribosome. In order to prevent protein from being transported to the cell membrane, NSP8 and NSP9 bind to the 7SL RNA at the Signal Recognition Particle (Mei-Yue Wang et.al,2020).
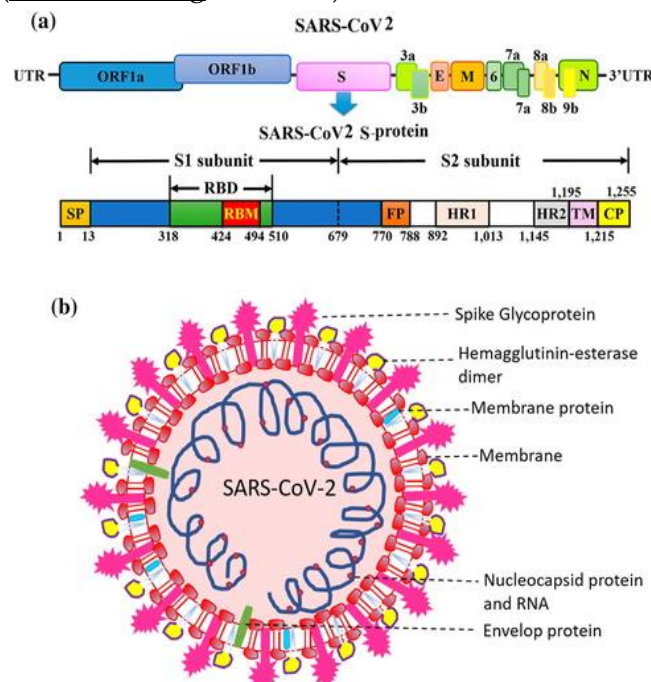
Figure 2: structure of sars-cov-2(mei-yue wang et al.,2020)

The transmembrane protein known as the spike, or S glycoprotein, has a molecular weight of around 150 kDa and is located in the virus's outer layer. By attracting the angiotensin-converting enzyme 2 (ACE2) produced in cells of the lower respiratory tract, S protein creates homotrimers that protrude from the viral surface and aids in the attachment of envelope viruses to host cells. The host cell's furin-like protease splits this glycoprotein into the S1 and S2 subunits. With the help of the receptor binding domain structure, part S1 determines the host viral range and cellular tropism, while part S2 mediates virus fusion in transmitting host cells.

The structural element of CoV that is structurally attached to the virus's nucleic acid is the nucleocapsid, also known as the N protein, which is found in the endoplasmic reticulum-Golgi area. The protein is engaged in procedures pertaining to the viral genome, the viral replication cycle, and the biological response of host cells to viral infections because the protein is attached to RNA. The N protein is also highly phosphorylated, which may cause structural alterations that increase its affinity for viral RNA.

The membrane protein, also known as the M protein, is another crucial component of this virus. It is the most structurally complex protein and affects how the virus's envelope is shaped. All other structural proteins can bind to this protein. By stabilising the N protein-

RNA complex inside the internal virion, binding with M protein aids in the stabilisation of nucleocapsids or N proteins and facilitates the completion of viral assembly. The final part of the SARS-CoV structure is the envelope, or E protein, which is the smallest protein and essential for the development and maturation of the virus (Indwiani Asttuti et al.,2020).

SARS-CoV2 binds to the ACE2 receptor, which is strongly expressed in the lower respiratory tract, including type II alveolar cells (AT2) of the lungs, upper oesophagus and stratified epithelial cells, as well as other cells like absorptive enterocytes from the ileum and colon, cholangiocytes, myocardial cells, kidney proximal tubule cells, and bladder urothelial cells. As a result, people who contract this virus not only endure respiratory issues like pneumonia that cause acute respiratory distress syndrome (ARDS), but also heart, renal, and digestive system difficulties (Indwiani et.al,2020)

The life cycle of coronaviruses begins when the virion binds to the host cell receptor via its spike protein S1 subunit and the complete life cycle of coronavirus is mentioned in Figure 3
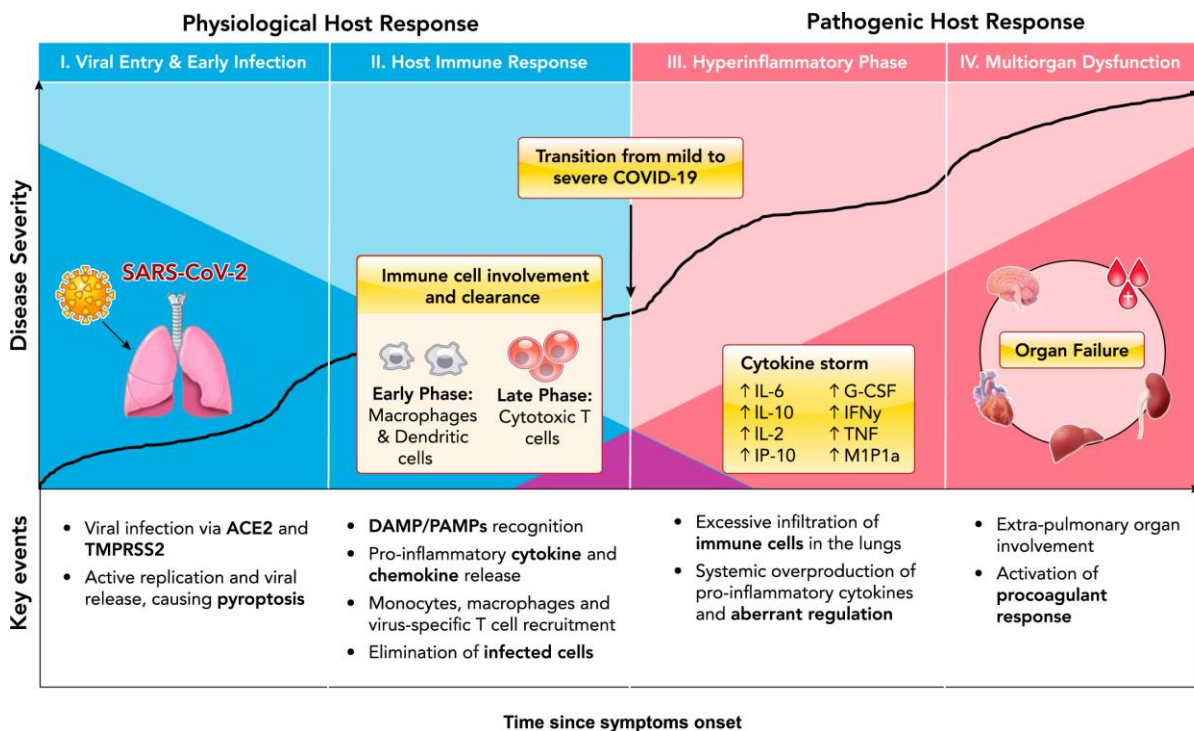
. **Figure 3: The Life Cycle of Coronaviruses (Glenna Burmer et al.,2020)**

PATHOGENESIS

SARS-CoV-2 infection in humans can cause moderate symptoms all the way up to serious respiratory failure. SARS-CoV-2 begins reproducing as soon as it binds to epithelial cells in the tract, moves down to the airways, and then reaches alveolar epithelial cells in the lungs. Strong reactivity could result from the SARS-CoV-2 virus's fast multiplication inside the lungs. Acute respiratory distress syndrome and respiratory failure are two of the most common causes of mortality in patients over the age of 60 and those with major underlying conditions, both of which increase the likelihood of both developing cytokine storm syndrome and death. In some COVID-19 cases, multiple organ failure has also been documented.

Patients with COVID-19 experience histopathology abnormalities primarily in the lungs. Histopathology examinations of the lungs of individuals with severe COVID-19 revealed

fibrin deposits, desquamation of pneumocytes, and bilateral distributed alveolar destruction. In certain instances, exudative inflammation was also visible. SARS-CoV-2 antigen was found in the upper airways, bronchiolar epithelium, submucosal gland epithelium, type I and type II pneumocytes, alveolar macrophages, and hyaline membranes in the lungs by immunohistochemistry assays (Ben Hu et.al,2021)

CURRENT SITUATION (EPIDEMIOLGY)

The severe acute respiratory syndrome coronavirus 2 (SARS-CoV-2) is the current cause of the COVID-19 pandemic, commonly referred to as the coronavirus pandemic. In Wuhan, China, the virus was initially discovered in December 2019. Early COVID-19 cases were frequently related to individuals who went to Wuhan's Huanan seafood wholesale market. It's probable that transfer from person to person was already occurring prior to this. The disease was given the COVID-19, or coronavirus disease 2019, designation by the World Health Organisation on February 11, 2020. Due to its close genetic resemblance to bat coronaviruses, it is thought to have zoonotic origins and may have developed from the bats-bone virus. The question of whether SARS-CoV-2 was transmitted directly from bats or indirectly via any intermediary hosts is still being investigated. The WORLD HEALTH ORGANISATION (WHO) proclaimed public health emergence of international concern on 30 January 2020 and later declared a pandemic on 11 march 2020.

The current SARS CoV 2 pandemic has a total of 181,155,202 confirmed cases as of June 28, 2021. The virus is responsible for 3,924,360 fatalities in all.

When there are no immune individuals in the community and no preventive measures are performed, epidemiological studies predict that each infection results in an average of 2.39 to 3.44 additional infections. Aerosols and respiratory droplets released during conversation, breathing, or other exhalations, as well as those brought induced by coughing or sneezing, are the main ways in which the virus is transmitted between people. It mostly enters human cells via attaching to angiotensin converting enzyme 2, a membrane protein that controls the renin-angiotensin system. (Ghebalwi et al.,2020)

Table 2: Epidemiological and clinical characteristics of SARS-CoV-2

Characteristics	COVID-19
Year of origin	December 2019
Virus strain	SARS-CoV-2
Original location	Wuhan, China
Conformed cases	770,875,433
Mortality rate	6,959,316
Natural reservoir host	Bat
Intermediate host	Pangolins
Genome length	29.9kb
Genus	Beta-COV lineage B
Incubation period	1-14 days
Basic reproduction number	2.2
Transmission	Respiratory droplets, close contact with diseased patients
Signs and symptoms	Fever, myalgia, cough, shortness of breath
Major complications	Pneumonia, severe acute respiratory distress syndrome, death
Transmission region	Globally
Predominant cellular receptor	ACE2

DIAGNOSIS AND TREATMENT
The importance of diagnosis is greatest in areas with a severe COVID19 epidemic, such as the United States of America, India, Brazil, and other nations. There are various diagnostic techniques, including:
RT PCR: Reverse transcription into DNA and polymerase chain reaction (PCR) amplification of particular DNA targets make up the laboratory procedure known as RT PCR (Reverse Transcription Polymerase Chain Reaction). could become as the most popular technique for diagnosing human cancer It is mostly employed to calculate the quantity of a certain RNA. This is accomplished using the real-time PCR or quantitative PCR (qPCR) technology, which uses fluorescence to monitor the amplification reaction. In both academic and medical settings, combined RT-PCR and qPCR are frequently employed for viral RNA quantification and gene expression investigation.

CT Scan
The CT Scan (Computed Tomography Scan) is a medical imaging technology used in radiology to provide fine-grained, noninvasive images of the body for diagnostic reasons. The individuals who perform CT scans are known as radiologists or radiography technologists. To measure X-ray attenuations by various tissues inside the body, CT scanners use a revolving x-ray tube and a row of detectors placed in the gantry. The computer-processed tomographic (cross-sectional) images (virtual slices) of a body are created from the many X-ray measurements acquired from various angles. Due to its negative effects, ionising radiation use can occasionally be restricted. While MRI is not recommended for patients with metallic implants or pacemakers, CT can be used in these cases.

Rapid Antigen Test (**RAT**)
Rapid Antigen Test (RAT), also known as Rapid Antigen Detection Test (RADT), is a quick diagnostic test appropriate for use at the point of care that quickly determines if an antigen is present or absent. It is frequently utilised for the identification of COVID-19's causative agent, SARS-CoV-2. In contrast to other medical tests that detect antibodies (antibody tests) or nucleic acids (nucleic acid tests), of either laboratory or point-of-care varieties, rapid tests are a form of lateral flow testing that detect protein. Rapid tests often produce results in 5 to 30 minutes, need little infrastructure or training, and offer significant cost advantages.

Drugs used in the treatment of SARS-CoV-2:
Remdesivir is an antiviral drug with broad-spectrum antiviral activity. On October 22, 2020, the FDA approved remdesivir under the brand name Veklury for the treatment of hospitalized COVID-19 patients 12 years of age and older.
Bamlanivimab (LY-CoV555) is a recombinant, neutralizing human IgG1 monoclonal antibody (mAb) directed against the spike protein of SARS-CoV-2. It was granted FDA **Emergency Use Authorization** (EUA) on November 9, 2020 for the treatment of recently diagnosed COVID-19. The FDA revoked the EUA for bamlanivimab monotherapy on April 16, 2021.

Casirivimab and Imdevimab (REGN-COV2) is a combination of two monoclonal antibodies that work to block the infectivity of the SARS-CoV-2 virus. It was granted FDA **Emergency Use Authorization** on November 21, 2020 for the treatment of mild to moderate COVID-19 in patients who are high risk for progression to severe COVID-19.

Bamlanivimab and Etesevimab (LY-CoV555 and LY-CoV016) is a combination of two monoclonal antibodies that work to block the infectivity of the SARS-CoV-2 virus. It was granted **Emergency Use Authorization** on February 9, 2021 for the treatment of mild to moderate COVID-19 in patients who are high risk for progression to severe COVID-19. On June 25, 2021, the ASPR announced the immediate pause of all distribution of bamlanivimab and etesevimab on a national basis until further notice.

Sotrovimab is a monoclonal antibody designed to block SARS-CoV-2 viral entry into healthy cells and clear infected cells in patients with COVID-19. It was granted **Emergency Use Authorization** on May 26, 2021 for the treatment of mild to moderate COVID-19 in patients who are high risk for progression to severe COVID-19.

Tocilizumab is an interleukin-6 receptor antagonist marketed under the brand name Actemra for the treatment of rheumatoid arthritis and other inflammatory conditions. It was granted **Emergency Use Authorization** on June 24, 2021 for the treatment of COVID-19 in hospitalized patients 2 years of age and older.

Herbal Remedies are also in practice by many people all over the world to prevent and control COVID-19. Herbal agents extracted from various plants, including *Echinacea*, *Cinchona*, *Curcuma longa*, and *Curcuma xanthorrhiza*, are considered for the treatment of COVID-19 (Nugraha et al., 2020).

Chapter-IV

Rationale of present research and Objectives

RATIONALE OF STUDY

Owing to its multiple pharmacological properties such as antioxidant, anti-inflammatory, anti-allergic, anti-diabetic, antiestrogenic, antibacterial, antiviral, neuroprotective activity and antitumor activities, curcumin has become the foremost candidate among phytochemical in recent years. Curcumin derivatives had also seen potential applications in treatment of various diseases. Due to issues such as bioavailability and absorption associated with Curcumin, its therapeutic benefits remained nascent. To overcome these limitations and to obtain compounds with improved efficacy and developing more active drugs efforts had been made by designing analogues and conjugates of Curcumin. Curcuminoids have a variety of potential biological benefits such as antioxidant, anti-inflammatory, anticancer, antibacterial, antifungal and antiviral activity. The antiviral activity of flavones is known from the 1990s.

Based on the above literature, it is clearly evident that curcumin and its derivatives possess wide range of biological activities. Further it is observed that these derivatives possess potent anticancer, antidiabetic, antioxidant and antimicrobial activities. Some of the curcumin derivatives have been investigated for their potential antimicrobial activities and they exhibited significant antibacterial, antifungal and anti viral properties in their scientific studies. (Hussain et al., 2020). Hence, in view of dire need for novel anti-viral agents to combat COVID-19 in the current study, various curcumin derivatives were selected and an attempt was made to perform the *in silico* studies on these derivatives and to assess their antiviral activity by molecular docking. Molecular analysis of the binding affinity of selected derivatives of curcumin was conducted by the docking method to determine the potential of these phytochemical derivatives as drug candidates for SARS COVID-19 virus.

AIM

The current study is aimed to perform *in silico* evaluation of some curcumin derivatives for anti-viral activity.

OBJECTIVES

▸ To draw the chemical structures of selected semisynthetic derivatives of curcumin using CHEM DRAW.
▸ To predict molecular properties of title compounds and bioactivity scores using MOLINSPIRATION.
▸ To assess the ADME properties, and toxicity of the title compounds using Swiss ADME and Pre ADMET web tools.
▸ To conduct docking studies on the selected curcumin derivatives using PATCH dock and to estimate their activity against SARs COV-2 virus.

Chapter-V

Methodology

Softwares and web tools:
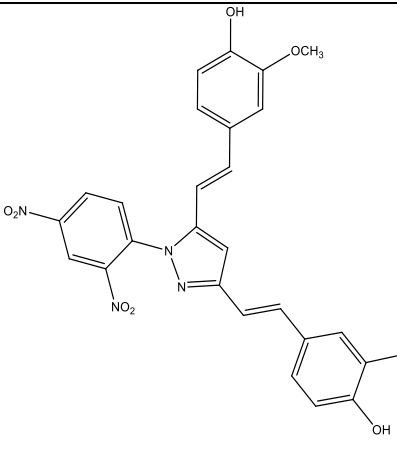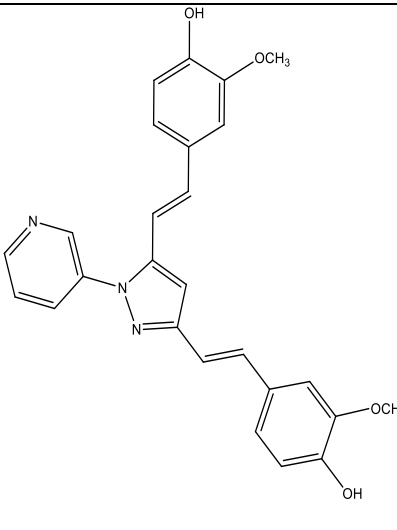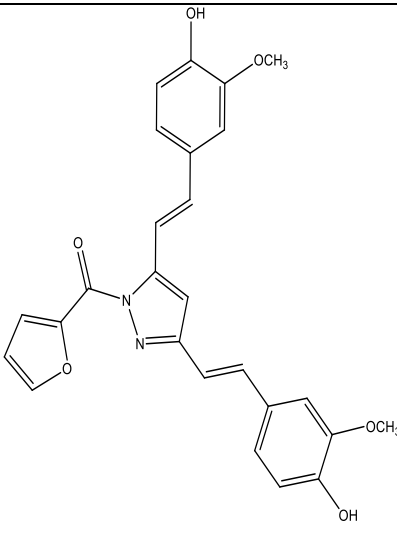
 Chem draw Ultra 2.0, Molinspiration(http://www.molinspiration.com), Swiss ADME (http://www.swissadme.ch/), Pre ADMET (http://preadmet.bmdrc.org/), Swiss target predictions and Patch Dock.

Preparation of Chemical Compounds library:
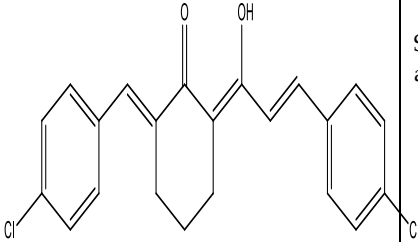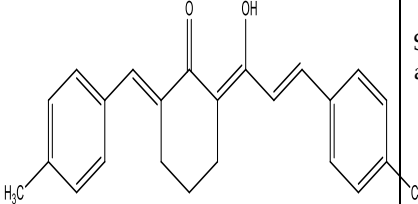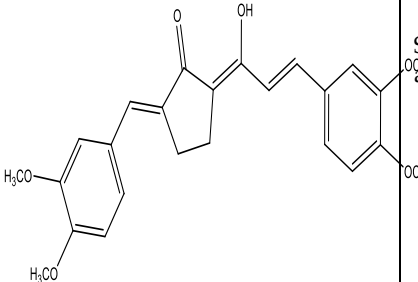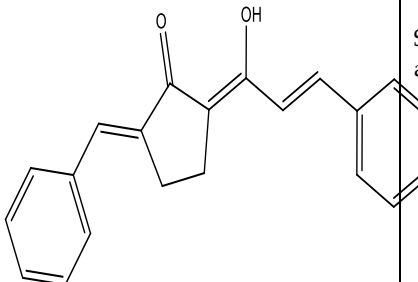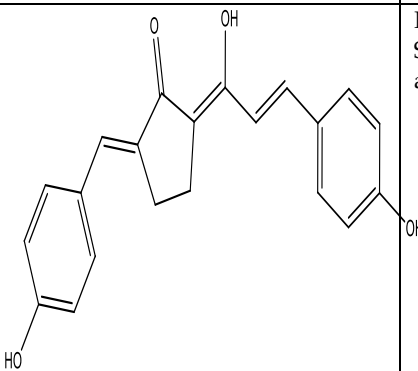
The structure of Curcuminoid-I was retrieved from the Chemical Compounds Database-Pubchem, and 45 compounds that had already been semi-synthesized as derivatives of curcumin were drawn using Chem Draw Ultra 12.0, with the molecular formula and IUPAC designations were recorded.
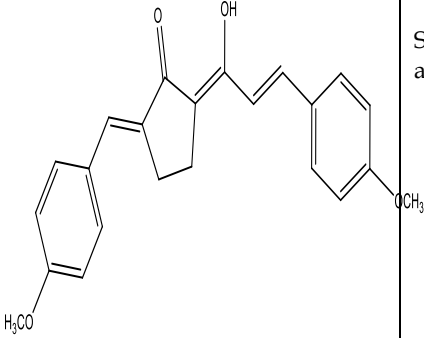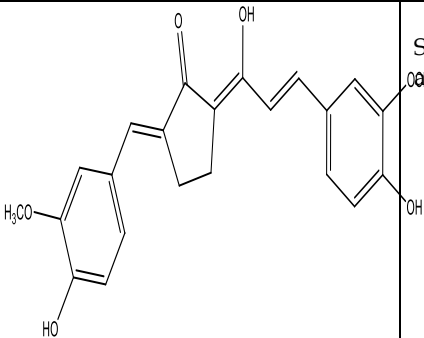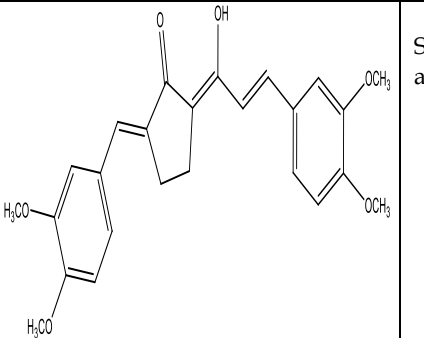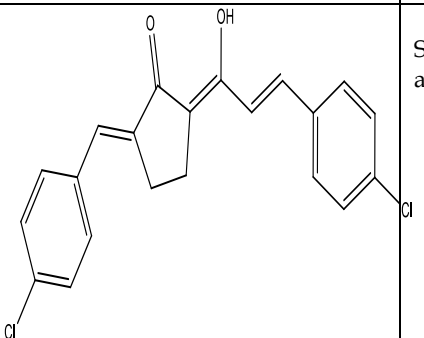
Table-3: Structures of Novel Curcumin Derivatives Drawn Using Chemdraw
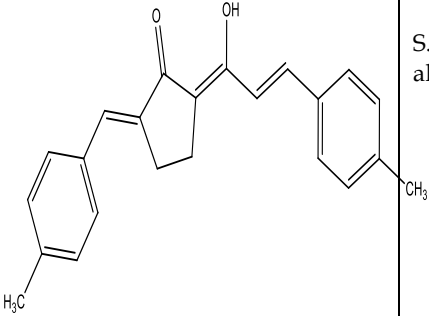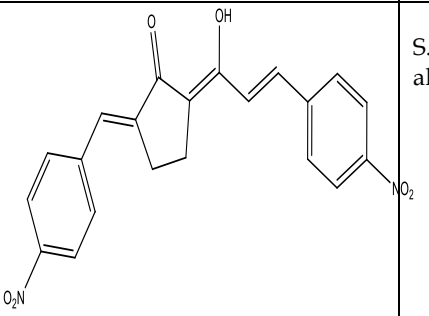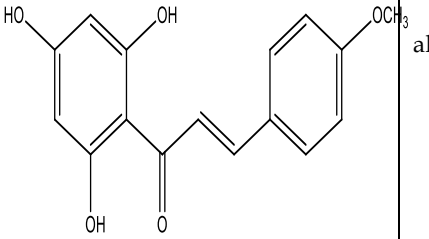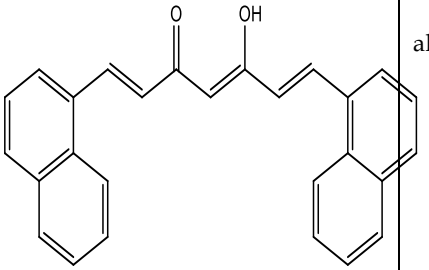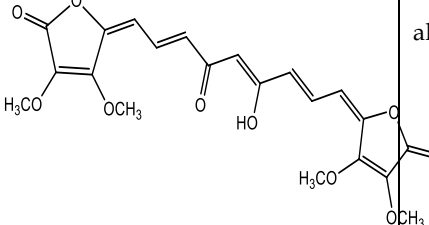
S.NO	NAME OF THE COMPOUND	MOLECULAR FORMULA	STRUCTURE OF THE COMPOUND	REFERENCE
01	(1E,6E)-5-hydroxy-1,7-bis(4-hydroxy-3-methoxyphenyl)hepta-1,6-dien-3-one	C21H22O6		Wing-Hin Lee et al., 2013
02	(1E,6E)-5-hydroxy-7-(4-hydroxy-3-methoxyphenyl)-1-(4-hydroxyphenyl)hepta-1,6-dien-3-one	C20H20O5		Wing-Hin Lee et al., 2013
03	(1E,6E)-5-hydroxy-1,7-bis(4-hydroxyphenyl)hepta-1,6-dien-3-one	C19H18O4		Wing-Hin Lee et al., 2013
04	4,4'-((1E,1'E)-(1-phenyl-1H-pyrazole-3,5-diyl)bis(ethene-2,1-diyl))bis(2-methoxyphenol)	C27H24N2O4		Othman A.Hamed et al.,2013
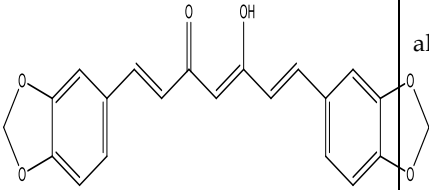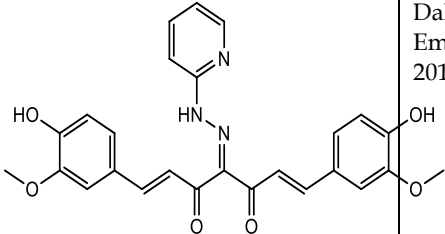
05	4,4'-((1E,1'E)-(1-(2,4-dinitrophenyl)-1H-pyrazole-3,5-diyl)bis(ethene-2,1-diyl))bis(2-methoxyphenol)	C27H22N4O8		Othman A.Hamed et al.,2013
06	4,4'-((1E,1'E)-(1-(pyridin-3-yl)-1H-pyrazole-3,5-diyl)bis(ethene-2,1-diyl))bis(2-methoxyphenol)	C26H23N3O4		Othman A.Hamed et al.,2013
7	(3,5-bis((E)-4-hydroxy-3-methoxystyryl)-1H-pyrazol-1-yl)(furan-2-yl)methanone	C26H22N2O6		Othman A.Hamed et al.,2013
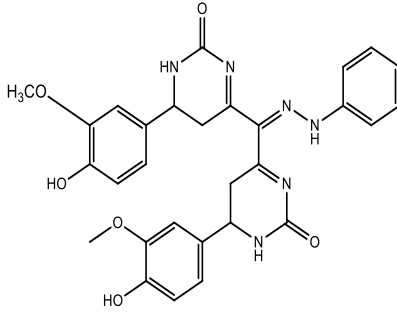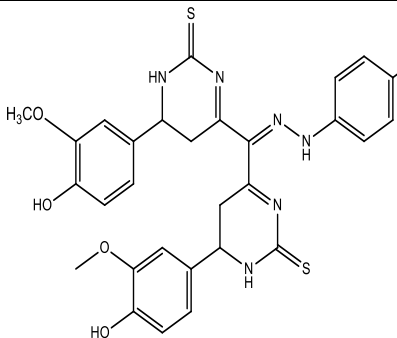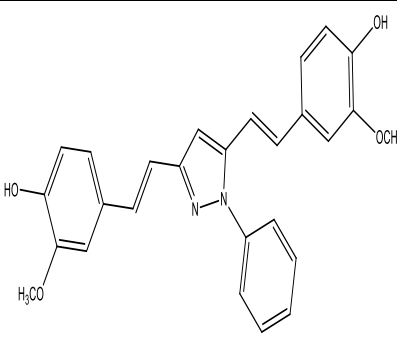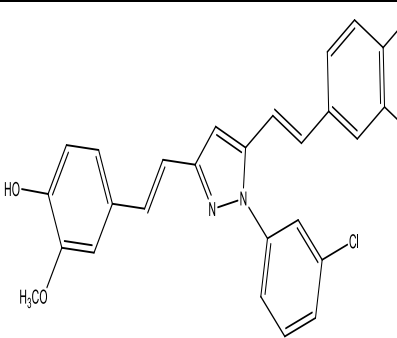
8	3,5-bis((E)-4-hydroxy-3-methoxystyryl)-1H-pyrazole-1-carbohydrazide	C22H22N4O5		Othman A.Hamed et al.,2013
9	(2Z,6E)-2-((E)-1-hydroxy-3-(4-hydroxyphenyl)allylidene)-6-(4-hydroxybenzylidene)cyclohexanone	C22H20O4		Kushwant S.Bhullar et al., 2013
10	(2E,6Z)-2-benzylidene-6-((E)-1-hydroxy-3-phenylallylidene)cyclohexanone	C22H20O2		Kushwant S.Bhullar et al., 2013
11	(2Z,6E)-2-((E)-1-hydroxy-3-(4-methoxyphenyl)allylidene)-6(methoxybenzylidene)cyclohexanone	C24H24O4		Kushwant S.Bhullar et al., 2013
12	(2Z,6E)-2-((E)-1-hydroxy-3-(4-hydroxy-3-methoxyphenyl)allylidene)-6-(4-hydroxy-3-methoxybenzylidene)cyclohexanone	C24H24O6		Kushwant S.Bhullar et al., 2013
13	(2E,6Z)-2-(3,4-dimethoxybenzylidene)-6-((E)-3-(3,4-dimethoxyphenyl)-1-hydroxyallyliden)cyclohexanone	C26H28O6		Kushwant S.Bhullar et al., 2013

14	(2E,6Z)-2-(4-chlorobenzylidene)-6-((E)-3-(4-chlorophenyl)-1-hydroxyallylidene)cyclo hexanone	C22H18Cl2O2		Kushwant S.Bhullar et al., 2013
15	(2Z,6E)-2-((E)-1-hydroxy-3-(p-tolyl)allylidene)-6-(4-methylbenzylidene)cyclohexanone	C24H24O2		Kushwant S.Bhullar et al., 2013
16	(2E,5Z)-2-(3,4-dimethoxybenzylidene)-5-((E)-3-(3,4-dimethoxyphenyl)-1-hydroxyallylidene)cyclo pentanone	C25H26O6		Kushwant S.Bhullar et al., 2013
17	(2E,5Z)-2-benzylidene-5-((E)-1-hydroxy-3-phenylallylidene)cyclop entanone	C21H18O2		Kushwant S.Bhullar et al., 2013
18	(2Z,5E)-2-((E)-1-hydroxy-3-(4-hydroxyphenyl)allylide ne)-5-(4-hydroxybenzylidene)cyc lopentanone	C21H18O4		Kushwant S.Bhullar et al., 2013
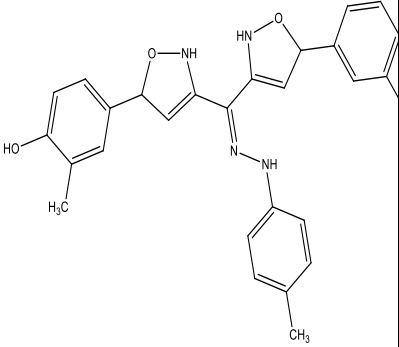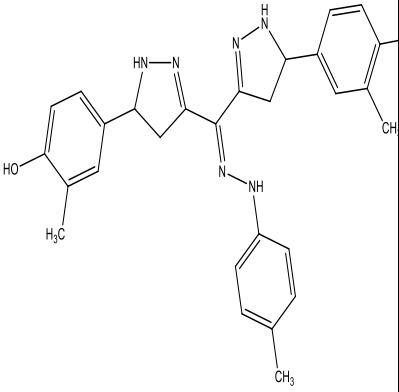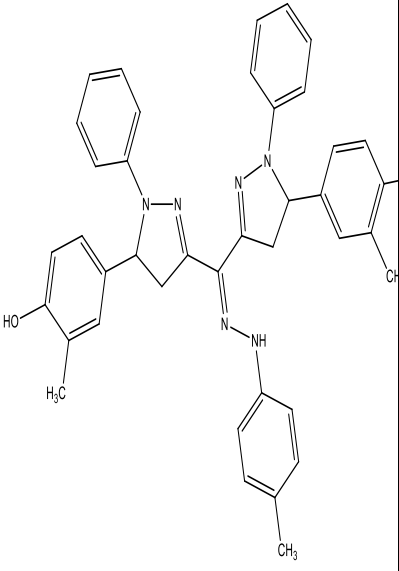
19	(2Z,5E)-2-((E)-1-hydroxy-3-(4-methoxyphenyl)allylidene)-5-(4-methoxybenzylidene)cyclopentanone	C23H22O4		Kushwant S.Bhullar et al., 2013
20	(2Z,5E)-2-((E)-1-hydroxy-3-(4-hydroxy-3-methoxyphenyl)allylidene)-5-(4-hydroxy-3-methoxybenzylidene)cyclopentanone	C23H22O6		Kushwant S.Bhullar et al., 2013
21	(2E,5Z)-2-(3,4-dimethoxybenzylidene)-5-((E)-3-(3,4-dimethoxyphenyl)-1-hydroxyallylidene)cyclopentanone	C25H26O6		Kushwant S.Bhullar et al., 2013
22	(2E,5Z)-2-(4-chlorobenzylidene)-5-((E)-3-(4-chlorophenyl)-1-hydroxyallylidene)cyclopentanone	C21H16Cl2O2		Kushwant S.Bhullar et al., 2013
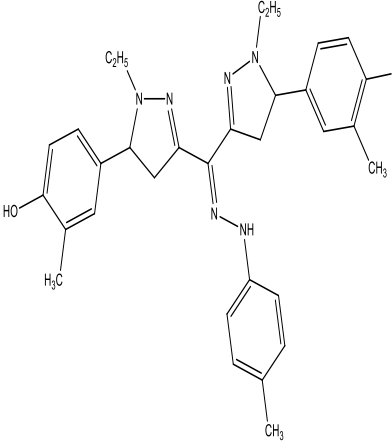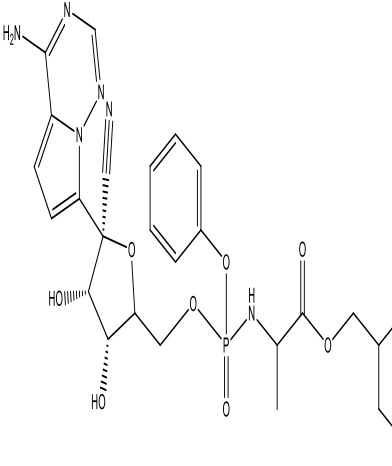
23	(2Z,5E)-2-((E)-1-hydroxy-3-(p-tolyl)allylidene)-5-(4-methylbenzylidene)cyclopentanone	C23H22O2		Kushwant S.Bhullar et al., 2013
24	(2Z,5E)-2-((E)-1-hydroxy-3-(4-nitrophenyl)allylidene)-5-(4-nitrobenzylidene)cyclopentanone	C21H16N2O6		Kushwant S.Bhullar et al., 2013
25	(E)-3-(4-methoxyphenyl)-1-(2,4,6-trihydroxyphenyl)prop-2-en-1-one	C16H14O5		Sokmen et al., 2016
26	(1E,4Z,6E)-5-hydroxy-1,7-di(naphthalen-1-yl)hepta-1,4,6-trien-3-one	C27H20O2		Sokmen et al., 2016
27	(5E,5'E)-5,5'-((2E,4Z,7E)-4-hydroxy-6-oxonona-2,4,7-triene-1,9-diylidene)bis(3,4-dimethoxyfuran-2(5H)-one)	C21H20O10		Sokmen et al., 2016

28	(1E,4Z,6E)-1,7-bis(benzo[d][1,3]dioxol-5-yl)-5-hydroxyhepta-1,4,6-trien-3-one	C21H16O6		Sokmen et al., 2016
29	1,7-Bis(4-hydroxy-3-methoxyphenyl)-4-(2-(p-tolyl)hydrazono)hepta-1,6-diene-3,5-dione	C28H26N2O6		Dalia R. Emam et al., 2017
30	1,7-Bis(4-hydroxy-3-methoxyphenyl)-4-(2-(pyridin-2-yl)hydrazono)hepta-1,6-diene-3,5-dione	C26H23N3O6		Dalia R. Emam et al., 2017
31	4-(2-(1,5-Dimethyl-3-oxo-2-phenyl-2,3-dihydro-1H-pyrazol-4-yl)hydrazono)-1,7-bis(4-hydroxy-3-methoxyphenyl)hepta-1,6-diene-3,5-dione	C32H30N4O7		Dalia R. Emam et al., 2017
32	4,4'-(6,6'-((2-(p-tolyl)hydrazono)methylene)bis(2-imino-2,3,4,5-tetrahydropyrimidine-6,4-diyl))bis(2-methoxyphenol)	C30H32N8O4		Dalia R. Emam et al., 2017

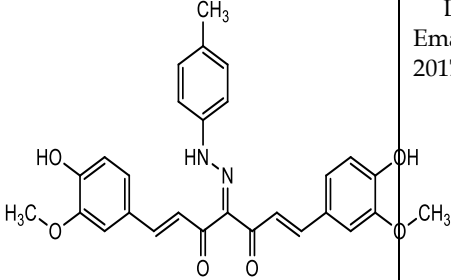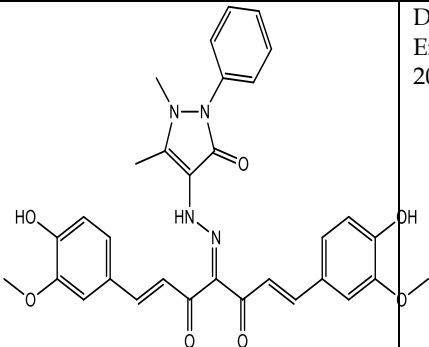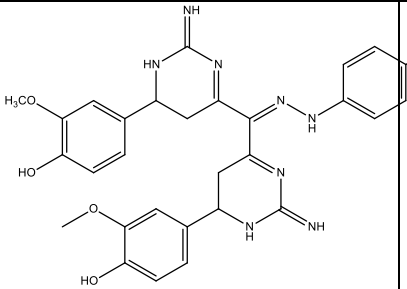| 33	4,4'-((2-(p-tolyl)hydrazono)methylene)bis(6-(4-hydroxy-3-methoxyphenyl)-5,6-dihydropyrimidin-2(1H)-one)	C30H30N6O6		Dalia R. Emam et al., 2017
34	4,4'-((2-(p-tolyl)hydrazono)methylene)bis(6-(4-hydroxy-3-methoxyphenyl)-5,6-dihydropyrimidine-2(1H)-thione)	C30H30N6O4S2		Dalia R. Emam et al., 2017
35	4,4'-((1E,1'E)-(1-phenyl-1H-pyrazole-3,5-diyl)bis(ethene-2,1-diyl))bis(2-methoxyphenol)	C27H24N2O4		Honnalagere Ramesh punnet et al.,2015
36	4,4'-((1E,1'E)-(1-(3-chlorophenyl)-1H-pyrazole-3,5-diyl)bis(ethene-2,1-diyl))bis(2-methoxyphenol)	C27H23ClN2O4		Honnalagere Ramesh punnet et al.,2015

37	4,4'-((1E,1'E)-(1-(2,4-dinitrophenyl)-1H-pyrazole-3,5-diyl)bis(ethene-2,1-diyl))bis(2-methoxyphenol)	C27H22N4O8		Honnalage re Ramesh punnet et al.,2015
38	4-(3,5-bis((E)-4-hydroxy-3-methoxystyryl)-1H-pyrazol-1-yl)benzonitrile	C28H23N3O4		Honnalage re Ramesh punnet et al.,2015
39	4,4'-((1E,1'E)-(1-(4-methoxyphenyl)-1H-pyrazole-3,5-diyl)bis(ethene-2,1-diyl))bis(2-methoxyphenol)	C28H26N2O5		Honnalage re Ramesh punnet et al.,2015
41	4,4'-((9E,9'E)-9,9'-((2-(p-tolyl)hydrazono)methylene)bis(5,6,7,8-tetrahydropyrido[2,3-b][1,4]diazocine-9,6-diyl))bis(2-methoxyphenol)	C40H40N8O4		Dalia R. Emam et al., 2017

42	4,4'-(3,3'-((2-(p-tolyl)hydrazono)methylene)bis(2,5-dihydroisoxazole-5,3-diyl))bis(2-methylphenol)	C28H28N4O4		Dalia R. Emam et al., 2017
43	4,4'-(3,3'-((2-(p-tolyl)hydrazono)methylene)bis(4,5-dihydro-1H-pyrazole-5,3-diyl))bis(2-methylphenol)	C28H30N6O2		Dalia R. Emam et al., 2017
44	4,4'-(3,3'-((2-(p-tolyl)hydrazono)methylene)bis(1-phenyl-4,5-dihydro-1H-pyrazole-5,3-diyl))bis(2-methylphenol)	C40H38N6O2		Dalia R. Emam et al., 2017

| 45 | 4,4'-(3,3'-((2-(p-tolyl)hydrazono)methylene)bis(1-ethyl-4,5-dihydro-1H-pyrazole-5,3-diyl))bis(2-methylphenol) | C32H38N6O2 | | Dalia R. Emam et al., 2017 |
| 46 | 2-ethylbutyl 2-(((((3R,4S,5S)-5-(4-aminopyrrolo[2,1-f][1,2,4]triazin-7-yl)-5-cyano-3,4-dihydroxytetrahydrofuran-2-yl)methoxy)(phenoxy)phosphoryl)amino)propanoate | C27H35N6O8P REMDESIVIR | | Dalia R. Emam et al., 2017 |

Prediction Of Molecular Properties

Molinspiration was used to test Lipinski's rule of five compounds and predict various physicochemical properties (http://www.molinspiration.com). The equation %ABS=109-(0.345TPSA) can be used to estimate the percentage absorption as well as other physicochemical properties that affect a molecule's biological activity, such as molecular weight, volume, molecular polar surface area (PSA), hydrogen bond acceptor/donor, log P, and number of rotatable bonds. Predicted bioactivity score values also show a compound's overall potential to be a therapeutic candidate.

ADME Properties

Various physicochemical, pharmacokinetic, drug-likeliness, GI absorption, BBB permeability, skin permeability, and toxicity features of substances were assessed utilising Swiss ADME and Pre ADMET web tools. (http://preadmet.bmdrc.org/), (http://www.swissadme.ch).

Intestinal absorption was demonstrated using Caco-2 permeability, and the Swiss-Boiled Egg model was utilised to show the potential of synthetic substances to penetrate the blood-brain barrier.

Small compounds can be processed by CYP and P-gp substrate in a synergistic manner to enhance tissue protection and serve as a key role in drug removal through metabolic bio transformation. 5 main isoforms (CYP1A2, CYP2C9, CYP2C19, CYP2B6, CYP3A4) are substrates for 50–90% of medicinal compounds. The interaction of compounds with

cytochromes P450 (CYP) was also predicted with Swiss ADME in order to assess the likelihood that the chemical will inhibit CYP and result in major drug interactions as well as to identify which isoforms are affected.

Toxicity prediction

PreADMET was used for the prediction of toxicity of compounds, in which hERG inhibition and Mutagenicity were predicted (http://preadmet.bmdrc.org/)

DOCKING OF CURCUMIN DERIVATIVES PATCHDOCK

The Critical Assessment of Prediction of Interactions (CAPRI) uses it as a prediction service. Image sequestration and object identification methods used in computer images serve as the basis for its algorithm. Here, a certain molecule's surface is divided into two patches based on the form of those surfaces. By using a segmentation method, the patches with hot spot residues are filtered out, leaving just the concave, convex, or flat surface patches that are typically observed. Once these patches have been found, they are superimposed in order to match the previously identified patches using shape matching algorithms like Geometric Hashing and Pose-Clustering matching. The last phase entails filtering out any complexes that exhibit unacceptable receptor atom to ligand atom penetration. Following this, the candidates that have been chosen are ranked complementarily based on geometric shape.

PREPARATION OF LIGAND:

Chemdraw Ultra12.0 is used to draw the ligand structure, and Chemdraw 3d Pro is used to minimise the energy, which is then stored as mol 2 form. The ligand must be saved in pdb form in order to be submitted to the patch dock programme. Using MGLtools, the ligand is transformed into pdb format.

PREPARATION OF PROTEIN:

The required protein pdb is downloaded from Protein Data Bank.

PROTEIN STRUCTURE DETAILS

Table 4: Protein Structure Details Of SARS Cov-2(Pdb Id: 6lu7)

Target enzyme	M ^{pro}
Organism	Severe acute respiratory syndrome coronavirus 2
Classification	Viral protein
Chain	A
Length	306 Amino acids
Molecular weight	34.51 kDa
Resolution	2.46 Å
Built in ligand	NO bound ligands

3D structure of target	
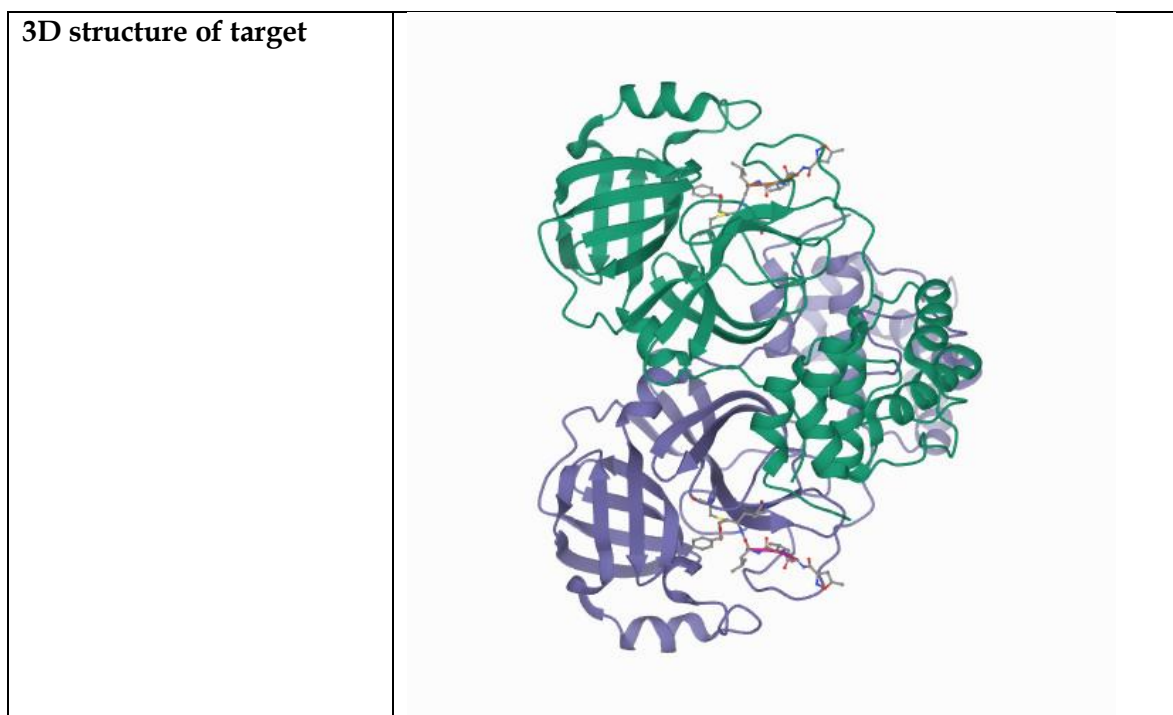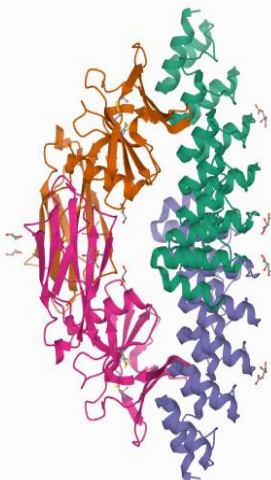
Table 5 : Protein Structure Details Of ACE-2 (Pdb Id:6moj)

Target enzyme	ACE-2
Organism	SYNTHETIC CONSTRUCT,HOMO SAPIENS
Classification	BIOSYNTHETIC PROTEIN
Chain	A
Length	231 Amino acids
Molecular weight	50.12 kDa
Resolution	2.43 Å
Built in ligand	1Xzn,1xCL,5xNAG
3D structure of target	

DOCKING PROCEDURE

The chosen receptor and ligands were docked by submitting them to the online, computerized molecular docking server Patch Dock. In order to receive the results, an email address was provided while keeping the clustering RMSD at 4.0 A°. The provided email address was used to receive and download the result.

Chapter-VI

Results

Prediction of Molecular Properties

Analysis of Lipinski's rule of five was carried out for derivatives by Molinspiration. Results showed that all derivatives except **L5,L32,L33,L34,L40,L43,L44** obeyed the five rules.

Table 6 Molecular Properties Of Curcumin Derivatives

S.NO	MOLECULAR WEIGHT	ROTATIONAL BONDS	HYDROGEN BOND DONORS	HYDROGEN ACCEPTORS	TPSA	LOG-P	VIOLATIONS	VOLUMES
L1	370.40	8	3	6	96.22	2.49	0	338.04
L2	340.38	7	3	5	86.99	2.69	0	312.50
L3	310.35	6	3	4	77.75	2.85	0	286.95
L4	440.50	7	2	5	76.75	5.57	1	401.44
L5	530.49	9	2	9	168.4	5.63	3	448.11
L6	441.49	7	2	6	89.64	4.71	0	397.28
L7	458.47	7	2	7	106.9	5.03	1	401.99
L8	422.44	6	4	7	131.8	2.50	0	372.71
L9	348.40	3	3	4	77.75	4.20	0	320.30
L10	316.40	3	1	2	37.30	5.15	1	304.27
L11	376.45	5	1	4	55.77	5.27	1	355.36
L12	408.45	5	3	6	96.22	3.83	0	371.39
L13	436.50	7	1	6	74.23	4.45	0	406.45
L14	385.29	3	1	2	37.30	6.51	1	331.34
L15	344.45	3	1	2	37.30	6.05	1	337.39
L16	422.48	7	1	6	74.23	3.94	0	389.65
L17	302.37	3	1	2	37.30	4.65	0	287.47
L18	334.37	3	3	4	77.75	3.69	0	303.50
L19	362.43	5	1	4	55.77	4.76	0	338.56
L20	394.42	5	3	6	96.22	3.33	0	354.59
L21	422.48	7	1	6	74.23	3.94	0	389.65
L22	371.26	3	1	2	37.30	6.00	0	314.54
L23	330.43	3	1	2	37.30	5.54	1	320.59
L24	300.36	03	1	6	37.30	2.90	0	306.84
L25	286.28	04	3	5	86.99	3.22	0	251.45

L26	376.45	05	1	2	37.30	6.33	01	352.69
L27	432.38	09	0	9	134.6	1.08	0	367.99
L28	364.35	05	1	6	74.23	4.15	0	312.56
L29	486.52	10	3	8	117.4	3.41	01	439.01
L30	473.49	10	3	8	130.3	2.53	0	418.30
L31	170.65	11	2	8	121.1	3.64	01	520.76
L32	566.62	08	6	9	184.0	2.91	03	501.50
L33	570.61	08	9	6	166.2	3.16	02	501.08
L34	587.71	08	5	7	127.3	2.00	01	499.88
L35	440.50	07	2	5	76.75	5.57	01	401.44
L36	474.94	07	1	2	76.75	6.44	01	414.98
L37	438.48	07	2	5	76.75	3.97	0	420.82
L38	453.50	07	2	9	99.02	5.11	01	407.23
L39	470.52	08	3	6	85.98	5.63	01	426.99
L40	696.81	08	9	6	157.8	7.14	03	631.22
L41	484.56	06	3	6	107.3	8.05	01	437.82
L42	482.59	06	5	5	113.6	7.24	01	445.14
L43	634.78	08	5	5	96.05	9.42	02	588.72
L44	538.70	8	5	3	37.30	8.39	2	512.63
L45	602.39	14	4	13	203.5	2.82	2	523.04
L46	598.64	14	10	02	163.1	4.65	02	540.13

From the **table 7**, results showed that Molecular weight of all compounds were found to be less than 500 daltons except **L5,L32,L33,L34,L40,L43,L44,L45** and expected that compounds can be easily transported, distributed and absorbed. All compounds except **L31,L45** have hydrogen bond acceptors ≤ 10,all compounds have hydrogen bond donors<5. Numbers of rotatable bonds of all compounds were found to be less than 10 for all compounds except for **L31, L45**, which is considered as a sign for good bioavailability.

Topological polar surface area (TPSA) is also a good indicator of bioavailability of compounds. All derivatives except **L5,L32,L33,L40** have shown TPSA in the range of **37.30-134A^O** and is well below the limit **140A^O**, LogP values are in the range of 0-5 except **L4,L5,L10,L11,L14,L15,L22,L35,L36,L38,L39,L40,L41,L42,L43,L44.** Molecular volume assesses the transport properties of molecules such as intestinal, blood brain barrier and heamatoencephalic barrier, **L31,L32,L33,L40,L43,L44,L45** showed volume more than 500 A^O.

 All compounds were found to obey lipinski's rule of five, none have violated more than one rule except **L5,L32,L33,L40,L44,L45** and this shows they possess good oral bioavailability.

Bioactivity scores of compounds:

Bioactivity scores of compounds against receptors such as G-protein coupled receptor, ion channels, kinase, nuclear receptor, enzyme and protease were predicted by Molinspiration. Results in the table- 8 displayed that all the compounds were found be in the range of **-5.0 to 5.0** which indicates that the compounds have ability to possess moderate to good activity towards biological targets.

Table 7: Bioactivity Scores Of Curcumin Derivatives

S.NO	GPCR LIGAND	ION CHANNEL	KINASE INHIBITOR	NUCLEAR RECEPTOR	PROTEIN INHIBITOR	ENZYME INHIBITOR
L1	0.09	-0.13	-0.26	0.11	0.00	0.34
L2	0.12	-0.12	-0.26	0.17	0.01	0.38
L3	0.17	-0.05	-0.26	0.24	0.08	0.45
L4	-0.03	-0.09	-0.02	-0.01	-0.06	0.01
L5	-0.15	-0.25	-0.20	-0.16	-0.22	-0.22
L6	0.09	-0.11	0.13	-0.04	-0.01	0.12
L7	-0.20	-0.34	-0.21	-0.11	-0.30	-0.11
L8	-0.09	-0.26	-0.06	-0.40	-0.11	0.10
L9	-0.20	-0.34	-0.39	0.14	-0.13	0.06
L10	-0.24	-0.40	-0.46	-0.04	-0.14	0.03
L11	-0.25	-0.41	-0.43	0.02	-0.17	-0.02
L12	-0.23	-0.37	-0.38	0.04	-0.20	0.01
L13	-0.23	-0.37	-0.38	-0.01	-0.18	-0.03
L14	-0.23	-0.37	-0.45	0.01	-0.16	- 0.01
L15	-0.27	-0.44	-0.47	0.01	-0.18	-0.03
L16	-0.36	-0.33	-0.38	-0.03	-0.19	-0.01
L17	-0.42	-0.33	-0.47	0.00	-0.18	0.04
L18	-0.35	-0.28	-0.40	0.12	-0.14	0.07
L19	-0.40	-0.35	-0.44	0.00	-0.18	-0.01
L20	-0.36	-0.32	-0.38	0.01	-0.21	0.02
L21	-0.36	-0.33	-0.38	- 0.03	-0.19	-0.01
L22	-0.39	-0.31	-0.45	-0.01	-0.18	0.01
L23	-0.43	-0.38	-0.47	-0.12	-0.20	-0.02
L24	-0.38	-0. 30	-0. 43	0.01	-0. 14	0.04
L25	-0. 12	-0. 06	-0. 20	0.10	-0. 22	0.08
L26	-0. 01	-0. 28	-0. 06	0.00	0.09	0.19
L27	0.06	-0. 19	-0. 16	0.08	0.16	0.23
L28	-0. 07	-0. 43	-0. 18	-0. 10	-0. 05	0.11
L29	-0. 23	-0. 40	-0. 35	-0 . 42	-0. 32	-0. 14
L30	-0. 17	-0. 37	-0. 17	-0. 42	-0. 34	-0. 09
L31	-0. 46	-1. 05	-0. 73	-0. 86	-0. 57	-0. 47
L32	-0. 19	-0. 59	-0. 49	-0. 72	-0. 25	-0. 40
L33	-0. 23	-0. 66	-0. 52	-0. 65	-0. 30	-0. 35
L34	-0. 38	-0. 65	-0. 61	-0. 75	-0. 43	-0. 47
L35	-0. 03	-0. 09	-0. 02	-0. 01	-0. 06	0.01
L36	-0. 04	-0. 11	-0. 05	-0. 03	-0. 12	-0. 03
L37	-0. 02	-0. 09	-0. 01	-0. 01	-0. 05	0.02
L38	-0. 03	-0. 07	-0. 00	-0. 02	-0. 04	0.01
L39	-0. 04	-0. 10	-0. 03	-0 . 00	-0. 06	0.01
L40	-0. 10	-0. 59	-0. 32	-0. 39	-0. 27	-0. 35
L41	-0. 20	-0. 21	-0. 12	-0. 06	-0. 20	-0. 09

L42	-0. 59	-0. 62	-0. 63	-0. 35	-0. 60	-0. 36
L43	-0. 61	-1. 47	-1. 20	-1. 08	-0. 57	-0. 85
L44	-0.10	-0.50	-0.40	-O.58	-0.37	-0.28
L45	0.27	-0.35	0.20	-0.48	-0.49	-0.38
L46	0.17	-0.35	0.16	-0.42	0.46	0.33

PREDICTION OF ADME Properties

Computations of important Absorption, distribution and metabolic properties of all the derivatives were performed by Swiss ADME, preADMET web tools.

Caco-2 model and MDCK cell are referred to as *in vitro* model for prediction of drug absorption, where the drug has been administered orally. Pre ADMET predicts the permeability of Caco-2 cell, MDCK cell, blood brain barrier, Human intestinal absorption, skin permeability and plasma protein binding. Caco-2 cells are derived from human colon adenocarcinoma which has multiple drug transport pathways. . Caco2 permeability of all compounds found to be between P_{Caco2}: **2-42 nm/sec**. This indicates that all compounds were found to have moderate to good permeability.

MDCK cell refers to Madin-Darby canine kidney cell. Since MDCK cells life span is less than the life span of Caco-2 cells, correlation between them is said to be high. MDCK cell system can be used as a good tool for rapid permeability screening. MDCK value of all compounds are between **0.04-135 nm/sec**.

The intestinal absorption is very important to find the potential candidate and PreADMET finds the absorption in percentage. All compounds were found to have High GI absorption except derivatives. **L29, L30, L31, L34, L38**

ABSORPTION PRPOERTIES OF CURCUMIN DERIVATIVES:

Table 8: Absorption Properties Of Curcumin Derivatives

COMPOUND NO	Caco-2 Permeability	MDCK	GI ABSORPTION	%ABSORPTION	SKIN PERMEABILITY
L1	19.1493	99.2289	HIGH	75.8041	-2.71334
L2	20.4404	32.6415	HIGH	78.988	-2.82113
L3	21.0963	4.31264	HIGH	82.245	-2.71302
L4	47.6303	0.46669	HIGH	82.5215	-2.03866
L6	42.5893	0.14519	HIGH	78.0988	-2.476
L7	27.2592	0.7020	HIGH	72.0988	-2.39553
L8	17.3019	0.0880	HIGH	63.504	-3.6884
L9	21.2654	0.348	HIGH	82.176	-2.65515
L10	39.2942	29.2974	HIGH	96.1315	-1.67138
L11	47.0552	0.09022	HIGH	89.759	-2.087
L12	20.5318	10.3765	HIGH	75.6316	-2.46504
L13	50.3049	1.63003	HIGH	83.39065	-2.3694
L14	44.0034	3.37317	HIGH	96.1315	-1.8157
L15	41.6376	6.030	HIGH	96.1315	-1.5502
L16	48.8359	1.6640	HIGH	83.3905	-2.49322
L17	35.3441	16.3478	HIGH	96.1315	-1.8279
L18	21.0979	0.3982	HIGH	82.17625	-2.91984
L19	44.5174	0.1164	HIGH	89.75	-2.21801
L20	20.1716	5.063	HIGH	75.8041	-2.66413
L21	48.8359	1.66404	HIGH	83.3906	-2.49322
L22	41.5866	1.0466	HIGH	96.1315	-1.94439

L23	38.2275	2.03862	HIGH	96.1315	-1.69266
L24	18.0828	0.056451	LOW	96.1315	-2.13497
L25	18.2354	6.75612	HIGH	78.98845	-3.38295
L26	41.8214	47.819	HIGH	96.1315	-1.48225
L27	46.673	1.00296	HIGH	62.5423	-3.64095
L28	33.9688	2.02531	HIGH	83.39065	-3.03869
L29	18.7075	94.3317	LOW	68.4763	-2.54308
L30	17.7696	93.3333	LOW	64.02925	-2.7006
L31	26.3017	0.043464	LOW	67.21705	-2.12269
L34	21.1897	3.81201	LOW	65.07115	-3.05295
L35	47.6303	0.466691	HIGH	82.52125	-2.03866
L36	33.0707	0.09045	HIGH	82.52125	-2.06259
L37	12.3847	0.043437	HIGH	82.52125	-2.20152
L38	30.5855	0.052286	LOW	74.8381	-2.02871
L39	28.7692	0.048085	HIGH	79.3369	-2.09089
L42	12.7355	0.044821	HIGH	71.95735	-2.77258
L43	18.868	0.045477	HIGH	69.79765	-2.57773
L46	2.17682	0.051410	LOW	52.7236	-6.98

Skin permeability is also predicted because of its crucial role in transdermal delivery of drug. All compounds have skin permeability in the range of **-1 to -3.68.** Plasma protein binding and Blood Brain Barrier permeation were predicted by the Swiss ADME. Compounds **L4,L6,L7,L9,L10,L14,L18,L22,L24,L26,L35,L36,L37,L38,L39,L43** found to possess strongly bound by plasma protein binding **(95-100 %)** and All the compounds except **L3,L9,L10,L15,L17,L19,L23,L28** have no penetration through blood brain barrier

Table -9: Distribution Properties Of Curcumin Derivatives

COMPOUND NO	BBB PERMEABILITY	%PLASMA PROTEIN BINDING	P-GP SUBSTRATE
L1	NO	86.122112	NO
L2	NO	87.789901	NO
L3	YES	91.499053	NO
L4	NO	100	NO
L6	NO	100	NO
L7	NO	96.093154	NO
L8	NO	91.324612	NO
L9	YES	99.348642	NO
L10	YES	94.435442	NO
L11	YES	92.308713	NO
L12	NO	92.076895	NO
L13	NO	90.282699	NO
L14	NO	100	NO
L15	YES	93.143579	NO
L16	NO	89.816763	NO
L17	YES	94.410724	NO
L18	NO	99.620487	NO

L19	YES	92.040555	NO
L20	NO	91.125142	NO
L21	NO	89.816763	NO
L22	NO	100	NO
L23	YES	93.03713	NO
L24	NO	98.558372	NO
L25	NO	93.151995	NO
L26	NO	100	YES
L27	NO	53.621023	NO
L28	YES	90.44	NO
L29	NO	87.48191	NO
L30	NO	87.484674	NO
L31	NO	93.285286	NO
L34	NO	85.280683	NO
L35	NO	100	NO
L36	NO	100	YES
L37	NO	96.630845	NO
L38	NO	100	NO
L39	NO	100	NO
L42	NO	94.703498	NO
L43	NO	99.927964	YES
L46	NO	5.303528	NO

Assessment of compound whether it is a P-gp substrate or not is important, because P-gp plays a very crucial role in preventing the intracellular accumulation of toxic compounds. From table 10, it was found that three compounds (**L-26,L36,L43**,) can be substrates of P-gp. Interactions of molecules with Cytochrome P450 (CYP) were also predicted because these CYP isoenzymes are crucial for drug elimination through phase I of metabolic biotransformation. Obtained results showed that compounds **L4,L9,L10,L11,L14,L16,L17,,L18,L19,L21,L22,L23,L24,L28,L31,L35,L37,L38,L42** were found to inhibit CYP2C19

Table :10-Metabolism Properties Of Curcumin Derivatives

COMPOUND NO	CYP1A2	CYP2C19	CYP2C9	CYP2D6	CYP3A4
L1	NO	NO	YES	NO	YES
L2	YES	NO	YES	NO	YES
L3	YES	NO	YES	NO	YES
L4	NO	YES	YES	NO	NO
L6	NO	YES	YES	NO	NO
L7	NO	NO	YES	NO	NO
L8	NO	NO	YES	NO	NO

L9	NO	YES	YES	NO	YES
L10	NO	YES	YES	NO	YES
L11	YES	YES	YES	NO	YES
L12	YES	NO	YES	NO	YES
L13	NO	NO	YES	NO	YES
L14	NO	YES	YES	NO	YES
L15	NO	NO	YES	NO	YES
L16	NO	YES	YES	NO	YES
L17	NO	YES	YES	NO	YES
L18	YES	YES	YES	NO	YES
L19	YES	YES	YES	NO	YES
L20	YES	NO	YES	NO	YES
L21	NO	YES	YES	NO	YES
L22	NO	YES	YES	NO	YES
L23	NO	YES	YES	NO	YES
L24	NO	YES	YES	NO	YES
L25	YES	NO	YES	NO	YES
L26	NO	NO	NO	NO	YES
L27	NO	NO	YES	NO	NO
L28	YES	YES	YES	NO	YES
L29	NO	NO	YES	NO	NO
L30	NO	NO	YES	NO	NO
L31	NO	YES	YES	NO	NO
L34	NO	NO	YES	NO	YES
L35	NO	YES	YES	NO	NO
L36	NO	NO	NO	NO	YES
L37	NO	YES	YES	NO	NO
L38	NO	YES	YES	NO	YES
L39	NO	NO	NO	NO	NO
L42	NO	YES	YES	NO	NO
L43	NO	NO	YES	NO	YES
L46	NO	YES	NO	YES	YES

TOXICITY PREDICTIONS

Toxicity studies like Mutagenicity, hERG inhibition were predicted. Some of the compounds like **L1,L2,L3,L4,L5,L6,L9,L12,L13,L20,L31,L35,L36** were found to be non-mutagens and many of compounds showed low to medium risk hERG inhibition.

Table :11-Toxicity Values Of Curcumin Derivatives

COMPOUND NO	PAINS	BRENKS	HERG INHIBITION	MUTAGENICITY
L1	0	1	Medium- risk	Non mutagen
L2	0	1	Medium- risk	Non mutagen
L3	0	1	Medium- risk	Non mutagen
L4	0	0	High-risk	Non mutagen
L6	0	0	Medium- risk	Non mutagen
L7	0	0	Medium- risk	Mutagen
L8	0	2	Medium- risk	Mutagen
L9	0	2	Medium- risk	Non mutagen
L10	0	2	Low-risk	Mutagen
L11	0	2	Medium- risk	Mutagen
L12	0	2	Medium- risk	Non mutagen
L13	0	2	Medium- risk	Non mutagen
L14	0	2	Medium- risk	Mutagen
L16	0	2	Medium- risk	Mutagen
L17	0	2	Low-risk	Mutagen
L18	0	2	Medium- risk	Mutagen
L19	0	2	Medium- risk	Mutagen
L20	0	2	Medium- risk	Non mutagen
L21	0	2	Medium- risk	Mutagen
L22	0	2	Medium- risk	Mutagen
L23	0	2	Medium- risk	Mutagen
L24	1	4	Medium- risk	Mutagen
L25	0	1	Medium-risk	Mutagen
L26	0	3	Low-risk	Mutagen
L27	0	4	Medium- risk	Mutagen
L28	0	3	Medium,-risk	Mutagen
L29	1	4	Medium- risk	Mutagen
L30	1	4	Medium-risk	Mutagen
L31	1	3	Medium-risk	Non mutagen
L34	0	4	High-risk	Mutagen
L35	0	0	High-risk	Non mutagen
L36	0	3	Medium- risk	Non mutagen
L37	0	0	Medium- risk	Mutagen
L38	0	2	Medium- risk	Mutagen
L39	0	0	Medium- risk	Mutagen
L42	0	1	High- risk	Mutagen
L43	0	1	High-risk	Non mutagen
L46	0	1	Ambiguous	non-mutagen

DOCKING STUDIES

Patchdock was used to calculate the atomic contact energy of molecules with macromolecular structure. Binding interactions of all compounds have shown strong Hydrogen bonding interaction and hydrophobic interaction with target proteins.

Docking of curcumin derivatives with SARS-CoV-2 (severe acute respiratory syndrome coronavirus 2)

Among all the derivatives compounds **L31,L7,L8,L4,L38,L35** have shown highest affinity with ACE value of **-387.22,-369.22,-360.81,-350.16,-333.43,-329.00** respectively , all the

compounds showed greater affinity than standard drug **REMEDISIVIR** (ACE=-205.91)
except **L25,L26 (Table)**

Table 12: Docking Scores

COMPOUND NO	SCORE	AREA	ACE	Interaction sites
L1	4058	561.60	-216.94	PRO(168A), THR(25A),THR(26A), HIS(164A),GLU(1666A), ASN(72A),GLN(69A),GLY(120A)
L2	3804	553.40	-270.13	ASN(72A),VAL(73A),GLY(71A) GLN(74A),GLY(120A)
L3	4028	457.80	-169.32	TRP(31A)
L4	4778	566.40	-350.16	TRY(237A),TYR(239A),MET(276A), THR(199A),ALA(275A)
L6	4808	600.80	-295.22	LEU(286A),LEU(287A),ARG(131A) LYS(13A),ASP(131A),ASN(238A),LEU(271A)
L7	4890	577.20	-369.22	THR(199A),TYR(237A),MET(276A) LEU(287A),LEU(271A)
L8	4382	647.30	-360.81	THR(21A),GLY(23A),THR(45A) LEU(61A),THR(25A),LYS(61A)
L9	4270	513.50	-235.63	VAL(202A),ILE(249A),PRO(252A) PRO(293A),PHE(294A),GLN(110A), THR(292A)
L10	4348	557.20	-244.35	VAL(3C),THR(24A),SER(46A)
L11	4562	612.10	-251.80	THR(24A),GLY(23A),THR(45A) SER(46A)
L12	4436	570.60	-257.81	VAL(3C),GLN(189A),THR(24A),THR(45A), SER(46A),ASN(146A),GLN(189A)
L13	4830	691.50	-287.99	VAL(3C),THR(24A),THR(45A),GLN(189A)
L14	4312	589.10	-266.85	VAL(3C),THR(24A), GLN(189A)
L15	4470	557.20	-258.46	GLN(110A),VAL(202A),IE(249A),PRO(293A), PHE(294A),VAL(297A)
L16	4762	663.00	-286.39	VAL(3C),THR(24A) ,THR(45A)
L17	3966	521.20	-236.51	VAL(3C),THR(24A) ,THR(45A)
L18	4516	564.50	-245.92	THR(24A) ,THR(45A)
L19	4384	580.80	-251.72	GLN(110A),ILE(249A),PRO(293A) VAL(297A),THR(292A),PHE(294A)
L20	4432	603.40	-258.20	VAL(3C),THR(24A), GLN(189A) ,THR(45A)
L21	4654	663.20	-264.05	TRP(31A),ALA(70A),VAL(73A) PRO(122A),GLU(14A),SER(123A)
L22	4424	573.30	-249.57	THR(24A) ,THR(45A)
L23	4470	578.30	-250.33	THR(24A) ,THR(45A),VAL(3C),SER(46A)
L24	4656	596.20	-258. 72	PRO (168A)
L25	3528	420.00	-189. 69	HIS(164A),GLU(164A)
L26	3526	418.00	-186. 00	THR(24A) ,THR(45A) ,ASN(142A) ,GLN(189A)
L27	5246	611.20	-218. 04	PRO(108A) ,GLN(110A) ,VAL(202A)
L28	4148	549.20	-266. 27	VAL(3C) ,GLN(189A) ,SER(46A) THR(25A) ,GLN(189A)
L29	4706	571.40	-228. 60	THR(25A) ,THR(46A) ,SER(46A)

				GLN(189A)
L30	5010	644.00	-289. 41	THR(24A) ,THR(45A) ASN(142A) .GLN(189A)
L31	5138	683.20	-387. 22	THR(24A) ,THR(45A) THR(21A) ,THR(25A)
L34	4404	602.60	-268. 27	TRP(31A) ,GLU(14A) ,GLY(120A) , LYS(97A) ,MET(17A)
L35	4852	662.00	-329. 00	THR(24A) ,MET(49A) ,LEU(50A) THR(25A)
L36	5030	633.10	-306. 63	THR(199A) ,TYR(237A) ,ASN(238A) TYR(239A)
L37	4962	630.60	-301. 41	VAL(3C) ,SER(46A) ,ASN(142A)
L38	5158	674.80	-333. 43	VAL(3C) ,SER(46A) ,ASN(142A)
L39	5022	734.80	-323. 68	VAL(3C) ,SER(46A) ,ASN(142A)
L42	5626	627.60	-287. 51	GLU(14A) ,GLN(19A) ,ALA(70A) , GLY(71A)
L43	4724	624.70	-312. 12	GLU(14A) ,GLN(19A) ,ALA(70A) GLY(71A)
L46	4426	581.60	-178.79	ALA (70), VAL (73), LYS (97), GLY (71), ASN (72)

DOCKING OF CURCUMIN DERIVATIVES WITH ACE-2 (SEVERE ACUTE RESPIRATORY SYNDROME CORONAVIRUS 2)

Among all the derivatives **L34,L31,L39,L43,L38,L36,L37,L42,L35** compounds have shown highest affinity with ACE value of **-445.82,-388,-339.98,-330.08,-326.13,-317,-310.03,-300.74,- 300** respectively , all the compounds showed greater affinity than standard drug **REMEDISIVIR** (**ACE=-244.56**) except **L3,L10,L11,L13,L17,L18,L25,L30 Table-15.**

Table 14: **Protein-6moj Docking Scores With Curcumin Derivatives**

| COMPOUND NO	SCORE	AREA	ACE	Interacting Amino acid residues
L1	4396	657.30	-246.57	GLU(25B),LEU(77A),THR(80A) THR(72A),MET(114A)
L2	5238	657.60	-251.16	GLU(25B),THR(80A),LEU(110A) ARG(111B),HIS(110B)
L3	4710	588.90	-221.11	GLU(25B),THR(80A),LEU(110A) ARG(111B),HIS(110B),ASP(110A)
L4	5580	802.30	-336.11	GLU(24B),GLU(25B),LEU(77A) THR(80A),LEU(110A),ARG(113A) ,MET(114A),THR(72A)
L6	4982	738.60	-288.48	PRO(23B),GLU(24B),THR(80A),HIS(110B)
L7	5254	769.30	-291.80	PRO(23B),GLU(24B),THR(80A),TYR(109B) THR(72A)
L8	5374	704.30	-275.42	GLU(25B),THR(80A),HIS(110B),MET (114A) LEU(25B),THR(72A),ARG(11B)
L9	4576	666.40	-276.81	PRO(23B),GLU(24B),THR(80A) PRO(107B),LEU(110A),MET(114A), TYR(109B)

L10	4662	614.80	-232.45	LEU(27B) ,THR(80A), PRO(107B), TYR(109B), HIS(110B),ARG(111B)
L11	4720	686.00	-226.93	GLU(25B),THR(80A) LEU(110A),TYR(109B) LEU(27B) ,LEU(26B),ASN(103A)
L12	4818	616.20	-247.17	GLU(25B),THR(80A), TYR(109B), LEU(26B),THR(72A)
L13	5546	715.00	-224.10	GLU(25B), LEU(27B),ARG(111B)
L14	5170	652.70	-249.04	THR(80A), TYR(109B), LEU(110A), ARG(111B)
L15	4378	613.80	-282.93	GLU(25B),THR(80A), TYR(109B), LEU(26B),THR(72A) HIS(110B),ARG(111B),LEU(18B)
L16	5726	745.20	-245.20	PRO(23B),GLU(24B),THR(80A),TYR(109B), LEU(110A) ,TYR(109B)
L17	4196	622.10	-236.89	GLU(25B),THR(80A), TYR(109B), LEU(26B),THR(72A) HIS(110B)
L18	4664	575.80	-207.34	GLU(25B), THR(80A), TYR(109B), GLU(24B), THR(72A)
L19	4610	613.90	-265.68	GLU(25B), THR(80A), THR(72A) HIS(110B),MET(114A)
L20	5340	677.80	-211.05	GLU (25B), THR (80A), GLU (24B), THR (72A), LEU (26B), ASN (103A) ARG (111B)
L21	5826	727.20	-249.98	GLU (25B), THR (80A), LEU (27B), TYR (109B), ARG (111B)
L22	4914	647.80	-246.80	LEU (27B), THR (80A), PRO (107B), LEU (110A) TYR (109B),
L23	4500	590.40	-257.14	GLU (25B), THR (80A), TYR (109B), ARG (111B), MET (114B), GLU (24B)
L24	4642	608.30	-257. 06	GLN (170B), VAL (182B) SER (184B), ASN (185B)
L25	4464	535.40	-228. 00	ARG (130B), MET (158A)
L26	4656	596.20	-258.72	ARG (130B), MET (158A)
L27	5726	727.60	-223. 45	GLN (170B), VAL (182B) SER (184B), ASN (185B)
L28	4698	637.00	-254. 00	GLN (170B), VAL (182B) SER (184B), ASN (185B)
L29	5194	659.10	-247. 50	GLN (170B), VAL (182B) SER (184B), ASN (185B)
L30	5230	639.40	-232. 60	GLN (170B), VAL (182B) SER (184B), ASN (185B)
L31	5654	840.20	-388. 00	GLN (170B), VAL (182B) SER(184B),ASN(185B)
L34	4706	758.20	-445. 82	ARG(120B)
L35	5256	764.80	-300. 00	GLN(170B),VAL(182B) SER(184B),ASN(185B)
L36	5678	820.60	-317. 00	PRO(23B),GLU(24B) THR(80A),PRO(107B) ASN(147A)
L37	6066	870.80	-310. 03	GLU(24B),THR(80A)

|				
				GLU(25B),ASN(103A),GLU(24B) GLU(25B),ASN(103A)
L38	5434	818.70	-326. 13	GLU(24B),THR(80A),GLU(25B) ASN(103A),GLU(24B),GLU(25B) ASN(103A)
L39	5250	759.60	-339. 98	GLU(24B),THR(80A) GLU(25B),ASN(103A),GLU(24B) GLU(25B),ASN(103A)
L42	5128	610.00	-300. 74	VAL(196A),THR(205A),PHE(207A) ,ASP(224A),HIS(225A),ALA(194A)
L43	5960	793.40	-330. 08	GLU(25B),LEU(77A),HIS(110B) MET(114A),THR(80A),TYR(109B) PHE(208B)
L46	5242	680	-244.56	ALA (70), VAL (73), LYS (97), GLY (71), ASN (72)

BEST BINDING AFFINITY MODES OF DOCKED COMPOUNDS WITH PROTEIN SARS -COV- 2: L31, L7, L8, L4
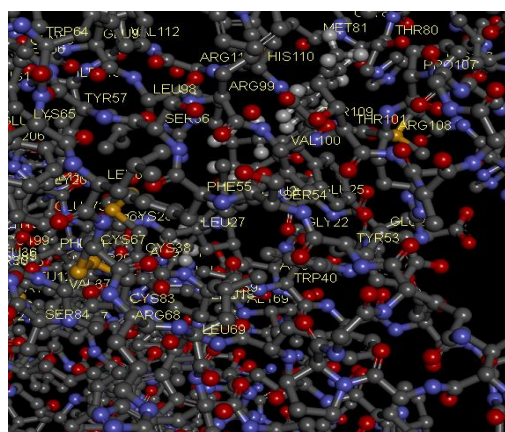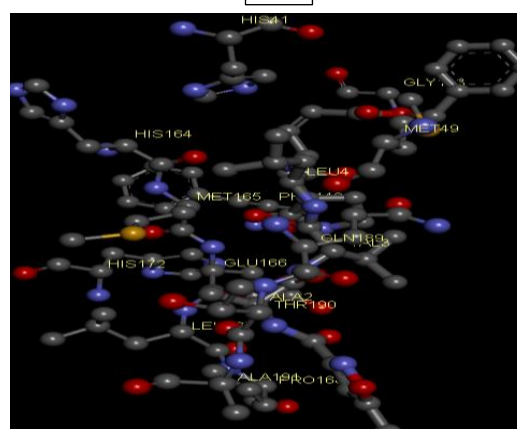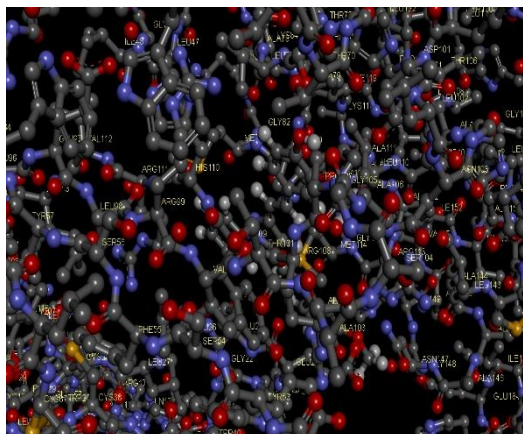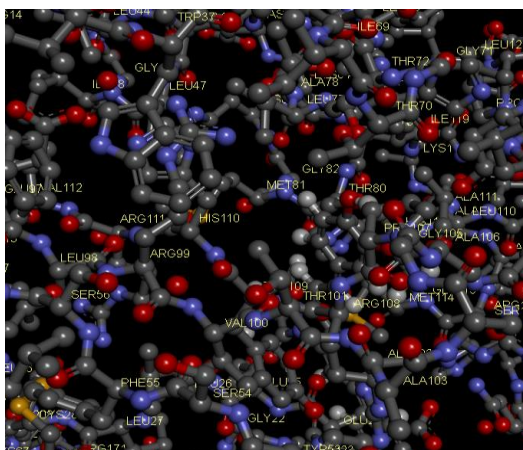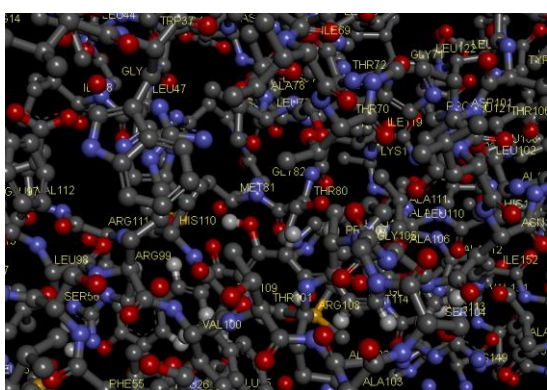

L31
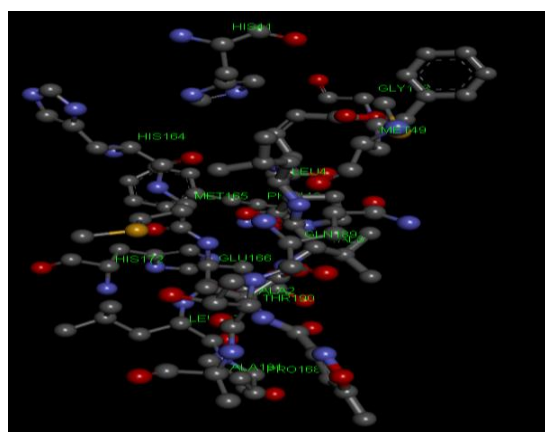
L7
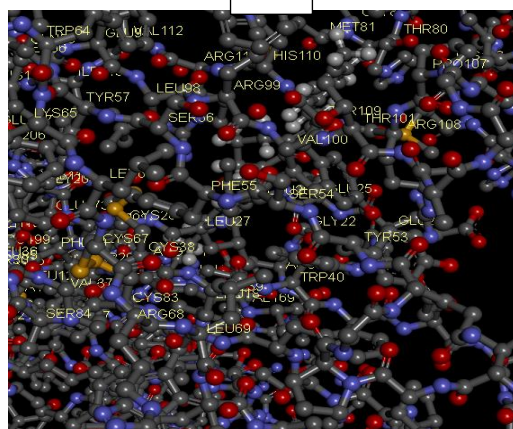
L8

L4

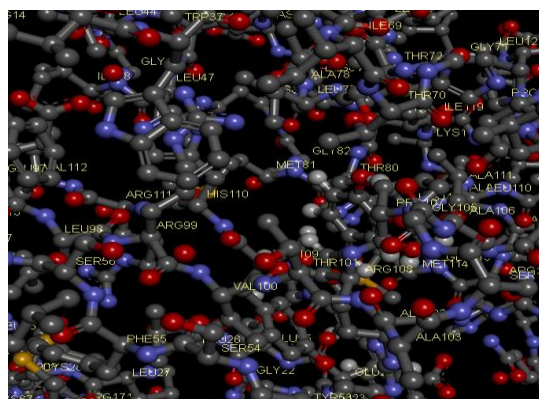**Figure 2: Best Binding Sites Of Compounds With Ace-2-L31,L34,L38,L39**

L34

L31

L38

L39

Chapter-VII

Discussion & Conclusion

DISCUSSION

In present work, curcumin derivatives were subjected to *in silico* studies. *In silico* studies has been gaining immense importance in the area of research and development because of its wide applications in evaluating bioactive substance and their physicochemical and pharmacokinetic properties. This helps to predict numerous failure that arise in the process of new drug development (Didier *et al.*, 2017).

About 40% of the candidate compound not being marketed is due to their poor biopharmaceutical properties (drug likeliness). Prediction of drug likeliness properties has been used immensely to filter out undesirable compounds in early phases of drug discovery (Venkatesh and lipper , 2000). By subjecting curcumin derivatives to the molinspiration web tool for predicting the molecular properties and bioactive scores, that all derivatives except **L5,L32,L33,L34,L40,L43,L44** obeyed the Lipinski's rule of five which indicates that compounds possess good oral bioavailability (Lipinski's *et al.*,1997) . Molecular weight of all compounds were found to be less than 500 daltons except **L5,L32,L33,L34,L40,L43,L44,L45** and expected that compounds can be easily transported, distributed and absorbed. Solubility in water can be estimated from the number of hydrogen bond donors in the molecule. compounds except **L31,L45** have hydrogen bond acceptors ≤ 10,all compounds have hydrogen bond donors, indicating that compound can penetrate and absorbs through the cell membrane. Bioactive scores of all compounds were found to be in the range of -5.0to 5.0 which indicates the binding affinity of the tested compound for the G protein ligand-coupled receptor (GPCR), ion channel modulation (ICM), kinase inhibition (KI), nuclear receptor ligand (NRL), protease inhibition (PI) and enzyme inhibition (EI).(Murugesan et al., 2021). These findings comes in harmony with previous reports on curcumin derivatives which states that these derivatives exhibit drug like properties and biological actions (Tomeh *et al.*,2019).

ADME properties of all compounds were predicted by Swiss ADME and pre ADMET online web tools.The absorption properties and permeability of all compounds were found where Caco-2 permeability of all compounds were in the range between Pcaco2:2-42nm.This indicates that all compounds were found to have moderate to good intestinal absorption. All compounds were found to have high absorption except **L24,L29,L31,L34,L36**. Further all Compounds **L4,L6,L7,L9,L10,L14,L18,L22,L24,L26,L35,L36,L37,L38,L39,L43** found to possess strongly bound by plasma protein binding **(95-100 %)** and All the compounds except **L3,L9,L10,L15,L17,L19,L23,L28** have no penetration through blood brain barrier and only three compounds were found to be substrate for P-gp. Metabolic properties are favourable since all the derivatives are expected not to inhibit more than three CYP 450 isoenzymes. These enzymes are involved in phase 1 biotransformation. Inhibition of these enzymes is major cause of pharmacokinetic-related drug-drug interactions. These findings come in accordance with the earlier scientific reports of Sandur et al., 2007, Tomeh et al., 2019 which stated that curcumin derivatives exhibit good absorption, distribution and metabolic properties.

Toxicity study was done by pre ADMET web tool. This online program predicts mutagenicity and hERG inhibition helps to predict cadiotoxicity. In the current study some of the compounds were found to non- mutagens and showed low to medium risk of hERG inhibition which supports the earlier computational studies on curcumin and other phytochemical derivatives (Munawar *et al.*,2020).

Molecular docking was performed in order to predict the preferred orientation of molecules to receptor/binding site/an enzyme. Patch dock was used to calculate the binding free energy of molecules with macromolecular structure. Binding interactions of all compounds

have shown strong hydrogen bonding interactions with target proteins (SARS- CoV- 2 and ACE-2).

ACE2 is a type 1 full-length membrane glycoprotein, which is expressed and active in most tissues. The highest expression of ACE2 was observed in the kidney, endothelium, lung and heart. ACE2 is related to the function of integrin, regardless of its angiotensinase activity. (Bosso et al.,2020). Docking studies of 6-MOJ with all compounds revealed that, compound L31 derivative have the highest binding affinity. All the compounds shown the greater affinity than the standard. This comes in parallel with the earlier reports on phytochemical derivatives (Basu *et al*.,2020).

SARS-CoV-2 main protease (M^{pro}) is one of two cysteine proteases necessary for viral replication and assembly. Docking studies of 6- LU7 revealed that the L34 showed highest binding affinity. These findings can be further supported with previous investigations, which stated that phytochemicals have potential role in combating viral diseases (Basu *et al*.,2020)

CONCLUSION

Based on the present computational study it is advantageous to focus on the curcumin derivatives to produce potent anti-viral drugs. It is clearly evident that curcumin derivatives have marked binding interactions with SARS CoV2 main protease and ACE-2 receptors. Hence the investigational curcumin derivatives have the probability to act as fruitful leads against COVID-19.

Chapter-VII

References

REFERENCES

1. A Hamed O, Mehdawi N, Abu Taha A, M Hamed E, A Al-Nuri M, S Hussein A. Synthesis and antibacterial activity of novel curcumin derivatives containing heterocyclic moiety. Iran J Pharm Res. 2013 Winter;12(1):47-56.

2. Astuti I, Ysrafil. Severe Acute Respiratory Syndrome Coronavirus 2 (SARS-CoV-2): An overview of viral structure and host response. Diabetes Metab Syndr. 2020 Jul-Aug;14(4):407-412. doi: 10.1016/j.dsx.2020.04.020.

3. Basu, A., Sarkar, A. & Maulik, U. Molecular docking study of potential phytochemicals and their effects on the complex of SARS-CoV2 spike protein and human ACE2. *Sci Rep* **10**, 17699 (2020). https://doi.org/10.1038/s41598-020-74715-4

4. Bhullar KS, Jha A, Youssef D, Rupasinghe HPV. Curcumin and Its Carbocyclic Analogs: Structure-Activity in Relation to Antioxidant and Selected Biological Properties. *Molecules*. 2013; 18(5):5389-5404. https://doi.org/10.3390/molecules18055389

5. Bosso M, Thanaraj TA, Abu-Farha M, Alanbaei M, Abubaker J, Al-Mulla F. The Two Faces of ACE2: The Role of ACE2 Receptor and Its Polymorphisms in Hypertension and COVID-19. Mol Ther Methods Clin Dev. 2020 Jun 25;18:321-327. doi: 10.1016/j.omtm.2020.06.017.

6. Chen SY, Chen Y, Li YP, Chen SH, Tan JH, Ou TM, Gu LQ, Huang ZS. Design, synthesis, and biological evaluation of curcumin analogues as multifunctional agents for the treatment of Alzheimer's disease. Bioorg Med Chem. 2011 Sep 15;19(18):5596-604. doi: 10.1016/j.bmc.2011.07.033.

7. Didier Rognan. The impact of in silico screening in the discovery of novel and safer drug candidates. Pharmacology and Therapeutics, 2017, 175, pp.47-66. ff10.1016/j.pharmthera.2017.02.034ff. ffhal-03543892f

8. Dnyaneshwar D. Subhedar, Mubarak H. Shaikh, Amol A. Nagargoje, Satish V. Akolkar, Sujit G. Bhansali, Dhiman Sarkar & Bapurao B. Shingate (2022) Amide-Linked Monocarbonyl Curcumin Analogues: Efficient Synthesis, Antitubercular Activity and Molecular Docking Study, Polycyclic Aromatic Compounds, 42:5, 2655-2671, DOI: 10.1080/10406638.2020.1852288

9. Emam DR, Alhajoj AM, Elattar KM, Kheder NA, Fadda AA. Synthesis and Evaluation of Curcuminoid Analogues as Antioxidant and Antibacterial Agents. *Molecules*. 2017; 22(6):971. https://doi.org/10.3390/molecules22060971

10. Emam DR, Alhajoj AM, Elattar KM, Kheder NA, Fadda AA. Synthesis and Evaluation of Curcuminoid Analogues as Antioxidant and Antibacterial Agents. *Molecules*. 2017; 22(6):971. https://doi.org/10.3390/molecules22060971

11. Ferreira LLC, Abreu MP, Costa CB, Leda PO, Behrens MD, Dos Santos EP. Curcumin and Its Analogs as a Therapeutic Strategy in Infections Caused by RNA Genome Viruses. Food Environ Virol. 2022 Jun;14(2):120-137.

12. Gheblawi M, Wang K, Viveiros A, Nguyen Q, Zhong JC, Turner AJ, Raizada MK, Grant MB, Oudit GY. Angiotensin-Converting Enzyme 2: SARS-CoV-2 Receptor and Regulator of the Renin-Angiotensin System: Celebrating the 20th Anniversary of the Discovery of ACE2. Circ Res. 2020 May 8;126(10):1456-1474. doi: 10.1161/CIRCRESAHA.120.317015.

13. H r, Puneeth & Hanumappa, Ananda & Sharath Kumar, Kothanahally & Rangappa, Kanchugarakoppal & Sharada, Angatahalli. (2016). Synthesis and antiproliferative

studies of curcumin pyrazole derivatives. Medicinal Chemistry Research. 25. 10.1007/s00044-016-1628-5.

14. Hasler, C. M and J. B. Blumberg. 1999. Symposiumon Phytochemicals, Biochemistry and Physiology. Journal of Nutrition, 129: 756 - 757.

15. https://hmsc.harvard.edu/online-exhibits/world-viruses/

16. https://www.lsbio.com/media/whitepapers/sars-cov-2-and-covid-19-pathogenesis-a-review

17. Hu, B., Guo, H., Zhou, P. *et al.* Characteristics of SARS-CoV-2 and COVID-19. *Nat Rev Microbiol* **19**, 141–154 (2021). https://doi.org/10.1038/s41579-020-00459-7

18. Hussain Y, Alam W, Ullah H, Dacrema M, Daglia M, Khan H, Arciola CR. Antimicrobial Potential of Curcumin: Therapeutic Potential and Challenges to Clinical Applications. Antibiotics (Basel). 2022 Feb 28;11(3):322. doi: 10.3390/antibiotics11030322.

19. Jaggi Lal, Sushil K. Gupta, D. Thavaselvam, Dau D. Agarwal, Synthesis and pharmacological activity evaluation of curcumin derivatives, Chinese Chemical Letters, 2016; 27(7): 1067-1072. ISSN 1001-8417, https://doi.org/10.1016/j.cclet.2016.03.032.

20. Khan MA, El-Khatib R, Rainsford KD, Whitehouse MW. Synthesis and anti-inflammatory properties of some aromatic and heterocyclic aromatic curcuminoids. Bioorg Chem. 2012 Feb;40(1):30-38. doi: 10.1016/j.bioorg.2011.11.004.

21. Kim, Bo & Park, Ji-Young & Jeong, Hyung & Kwon, Hyung-Jun & Park, S.C. & Lee, In chul & Ryu, Young & Lee, Woo. (2018). Design, synthesis, and evaluation of curcumin analogues as potential inhibitors of bacterial sialidase. Journal of Enzyme Inhibition and Medicinal Chemistry. 33. 1256-1265. 10.1080/14756366.2018.1488695.

22. Lee WH, Loo CY, Bebawy M, Luk F, Mason RS, Rohanizadeh R. Curcumin and its derivatives: their application in neuropharmacology and neuroscience in the 21st century. Curr Neuropharmacol. 2013 Jul;11(4):338-78. doi: 10.2174/1570159X11311040002.

23. Lipinski, C.A., 2000. Drug-like property and the cause of poor solubility and poor permeability. J. Pharm. Toxicol. Meth. 44, 235–249.

24. Liu B, Xia M, Ji X, Xu L, Dong J. Synthesis and antiproliferative effect of novel curcumin analogues. Chem Pharm Bull (Tokyo). 2013;61(7):757-63. doi: 10.1248/cpb.c13-00295.

25. Munawar S, Windley MJ, Tse EG, Todd MH, Hill AP, Vandenberg JI, Jabeen I. Experimentally Validated Pharmacoinformatics Approach to Predict hERG Inhibition Potential of New Chemical Entities. Front Pharmacol. 2018 Sep 19;9:1035. doi: 10.3389/fphar.2018.01035.

26. Murugesan S, Kottekad S, Crasta I, Sreevathsan S, Usharani D, Perumal MK, Mudliar SN. Targeting COVID-19 (SARS-CoV-2) main protease through active phytocompounds of ayurvedic medicinal plants - Emblica officinalis (Amla), Phyllanthus niruri Linn. (Bhumi Amla) and Tinospora cordifolia (Giloy) - A molecular docking and simulation study. Comput Biol Med. 2021 Sep;136:104683. doi: 10.1016/j.compbiomed.2021.104683.

27. Nugraha RV, Ridwansyah H, Ghozali M, Khairani AF, Atik N. Traditional Herbal Medicine Candidates as Complementary Treatments for COVID-19: A Review of Their Mechanisms, Pros and Cons. Evid Based Complement Alternat Med. 2020 Oct 10;2020:2560645. doi: 10.1155/2020/2560645.

28. Parasuraman A. Subramani, Kalpana Panati, Veeranjaneya R. Lebaka, Dharaneeswara D. Reddy, Venkata Ramireddy Narala, Chapter 21 - Nanostructures for Curcumin Delivery: Possibilities and Challenges, Editor(s): Alexandru Mihai Grumezescu, Nano- and Microscale Drug Delivery Systems, Elsevier, 2017, Pages 393-418.

29. Puneeth, H. R.; Chandrashekariah, S. A. Antioxidant and hypoglycemic effects of curcumin pyrazole derivatives. *Int J Pharm Pharm Sci* **2015**, *7*, 244-249.

30. Ramendra K. Singh, Diwakar Rai, Dipti Yadav, A. Bhargava, J. Balzarini, E. De Clercq, Synthesis, antibacterial and antiviral properties of curcumin bioconjugates bearing dipeptide, fatty acids and folic acid, European Journal of Medicinal Chemistry, 2010; 45(3): 1078-1086. https://doi.org/10.1016/j.ejmech.2009.12.002.

31. Sandur S.K., Pandey M.K., Sung B., Ahn K.S., Murakami A., Sethi G., Limtrakul P., Badmaev V., Aggarwal B.B. Curcumin, demethoxycurcumin, bisdemethoxycurcumin, tetrahydrocurcumin and turmerones differentially regulate anti-inflammatory and anti-proliferative responses through a ROS-independent mechanism. *Carcinogenesis.* 2007;28:1765–1773. doi: 10.1093/carcin/bgm123.

32. Singh A, Singh JV, Rana A, Bhagat K, Gulati HK, Kumar R, Salwan R, Bhagat K, Kaur G, Singh N, Kumar R, Singh H, Sharma S, Bedi PMS. Monocarbonyl Curcumin-Based Molecular Hybrids as Potent Antibacterial Agents. ACS Omega. 2019 Jul 5;4(7):11673-11684. doi: 10.1021/acsomega.9b01109.

33. Sökmen, M., Akram Khan, M. The antioxidant activity of some curcuminoids and chalcones. *Inflammopharmacol* **24**, 81–86 (2016). https://doi.org/10.1007/s10787-016-0264-5

34. Tomeh MA, Hadianamrei R, Zhao X. A Review of Curcumin and Its Derivatives as Anticancer Agents. Int J Mol Sci. 2019 Feb 27;20(5):1033. doi: 10.3390/ijms20051033.

35. Venkatesh, S., Lipper, R.A., 2000. Role of the development scientist in compound lead selection and optimization. J. Pharm. Sci. 89, 145–154.

36. Wang M-Y, Zhao R, Gao L-J, Gao X-F, Wang D-P and Cao J-M (2020) SARS-CoV-2: Structure, Biology, and Structure-Based Therapeutics Development. *Front. Cell. Infect. Microbiol.* 10:587269. doi: 10.3389/fcimb.2020.587269

37. Yolles M, Frieden R. Viruses as Living Systems—A Metacybernetic View. *Systems.* 2022; 10(3):70. https://doi.org/10.3390/systems10030070

38. Yuan X, Li H, Bai H, Su Z, Xiang Q, Wang C, Zhao B, Zhang Y, Zhang Q, Chu Y, Huang Y. Synthesis of novel curcumin analogues for inhibition of 11β-hydroxysteroid dehydrogenase type 1 with anti-diabetic properties. Eur J Med Chem. 2014 Apr 22;77:223-30. doi: 10.1016/j.ejmech.2014.03.012.